Simulation of direct transport of x-ray photons using the general purpose Monte Carlo code MCSHAPE: main features and recent developments

Jorge E. Fernández[1,2] and Viviana Scot[1]

1) Laboratory of Montecuccolino-DIN Alma Mater Studiorum University of Bologna, Italy

2) Istituto Nazionale di Fisica Nucleare (INFN)

Summary

- Introduction
- Unbiased Monte Carlo simulation of the Compton Profile
- Deterministic vs Monte Carlo codes for transport calculations of line width effects
- Electron contributions to photon transport
- Conclusions

Introduction

- Deterministic and Monte Carlo techniques compete to provide the best description of transport problems.
- However, many times they demonstrate to be complementary.
- This talk offers some examples from our experience in photon transport which illustrate the close cooperation between these two approaches to treat properly the physics of the collisions.
- The following examples show recent refinement in the description of the interactions in MCSHAPE but also useful for deterministic codes.

CHARACTERISTICS OF THE CODE MCSHAPE

- Photon transport
- Arbitrary polarization state of the source
- Multi-layer multi-component homogeneous targets
- Monochromatic or polychromatic source
- State of art description of the photon interactions in the x-ray regime: Rayleigh and Compton scattering, and photoelectric ionization followed by radiative relaxation
- Compton profile (for Compton scattering)
- Full description of the polarization state
- N-collisions
- 1D and 3D versions

PHOTON DIFFUSION IS DESCRIBED BY A "VECTOR" TRANSPORT EQUATION (THE 1-D EQUATION IS SHOWN HERE)

$$\eta \frac{\partial}{\partial z} \vec{f}^{(S)}(z, \vec{\varpi}, \lambda) = -\mu(\lambda) \vec{f}^{(S)}(z, \vec{\varpi}, \lambda)$$

$$+ \int_{4\pi} d\varpi' \int_0^{\infty} d\lambda' \mathrm{U}(z) \mathrm{H}^{(S)}(\vec{\varpi}, \lambda, \vec{\varpi}', \lambda') \vec{f}^{(S)}(z, \vec{\varpi}', \lambda')$$

$$+ \delta(z) \vec{S}^{(S)}(\vec{\varpi}, \lambda)$$

where

$$\overline{f} = \begin{bmatrix} I(z, \overline{\omega}, \lambda) \\ Q(z, \overline{\omega}, \lambda) \\ U(z, \overline{\omega}, \lambda) \\ V(z, \overline{\omega}, \lambda) \end{bmatrix}$$

VECTOR TRANSPORT EQUATION (CONT.)

where

$$\mathrm{H}^{(S)}(\vec{\varpi}, \lambda, \vec{\varpi}', \lambda') = \mathrm{L}^{(S)}(\pi - \Psi)\mathrm{K}^{(S)}(\vec{\varpi}, \lambda, \vec{\varpi}', \lambda')\mathrm{L}^{(S)}(-\Psi')$$

= kernel matrix in the meridian plane of reference

= scattering matrix in the scattering plane of reference

IMPORTANT PROPERTIES OF THE "VECTOR" TRANSPORT EQUATION

- Describes the evolution of the full polarization state (not only the intensity of the beam)
- Is linear (for the Stokes representation)
- Requires the simultaneous solution of the whole set of transport equations
- Cannot be transformed in a scalar equation !! (due to the coupling in the scattering term)

WHY POLARIZATION?

Polarization state → **wave nature of photons**

By considering polarization we improve the model of photon diffusion

↓

a good approximation in many cases, but not for phenomena that are influenced by their wave properties

TWO RELEVANT ASPECTS

- A collision always changes the polarization state
- The angular distribution for scattered unpolarized and polarized photons is very different

Summary

- Introduction
- Unbiased Monte Carlo simulation of the Compton Profile
- Deterministic vs Monte Carlo codes for transport calculations of line width effects
- Electron contributions to photon transport
- Conclusions

Unbiased Monte Carlo simulation of the Compton Profile

This example shows how a deterministic calculation has been used to correct a biased Monte Carlo algorithm widely adopted to simulate the Compton profile.

The proper calculation is included in MCSHAPE

ELSEVIER

Available online at www.sciencedirect.com

ScienceDirect

Nuclear Instruments and Methods in Physics Research B 263 (2007) 209 213

NIM B
Beam Interactions with Materials & Atoms

www.elsevier.com/locate/nimb

Unbiased Monte Carlo simulation of the Compton profile

J.E. Fernandez [a,b,*], V. Scot [b]

[a] *National Institute of Nuclear Physics (INFN), Italy*
[b] *National Institute for Physics of Matter (CNR/INFM) and Laboratory of Montecuccolino-DIENCA, Alma Mater Studiorum University of Bologna, Bologna, Italy*

Compton profile

- It is the broadening of the Compton peak
- It is produced by the momentum distribution of the electrons in the atom
- it can be measured quite precisely in synchrotron facilities

Biased Algorithm

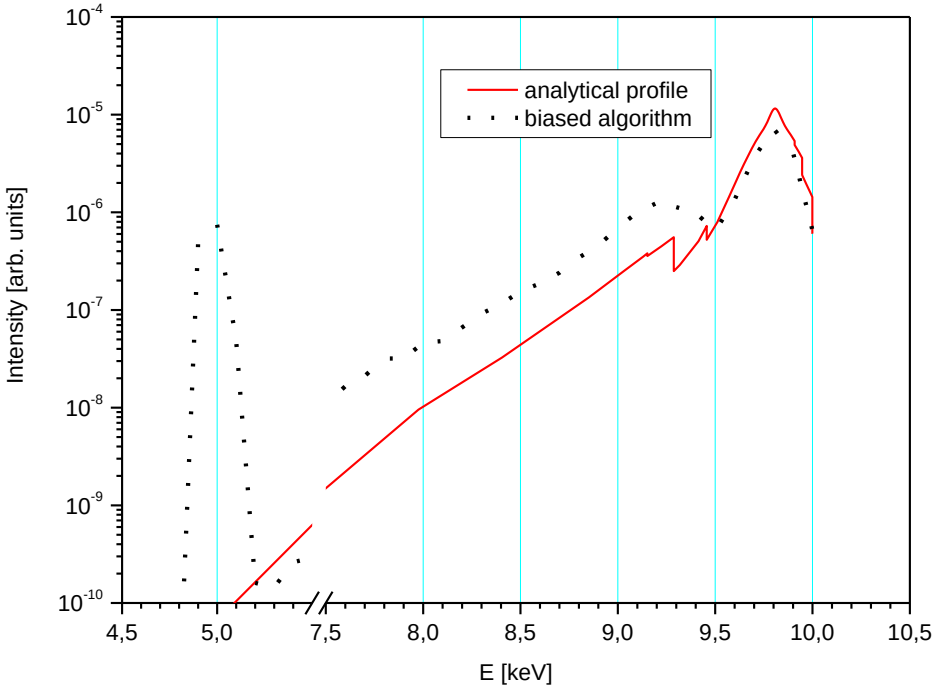

It was discovered a biased behaviour in Compton profile MC simulation (at low energies) when using the standard algorithm by Namito[1] (used by both, EGS and MCNP)

The bias was responsible for:

- the creation of a false peak in correspondence with the low energy tail of the profile
- a wrong Compton profile at low energies

[1] Y.Namito, S.Ban, H.Hirayama,NIM A 349 (1994) 489.

Reason for the bias

Wrong sampling of the atomic sub-shells:

$$\frac{n_i}{\left(\sum_{i=1}^{shellnumber} n_i\right)}$$

sub-shells were assumed complete

i.e. having $\boxed{n_i}$ electrons

Unbiased sampling

Correct sampling of the atomic sub-shells:

$$\frac{n_i \int_{-\infty}^{Q_{i,\max}} J_i(Q)dQ}{\sum_{i=1}^{shellnumber} n_i \int_{-\infty}^{Q_{i,\max}} J_i(Q)dQ}$$

sub-shells now are assumed incomplete

i.e. having $n_i \int_{-\infty}^{Q_{i,\max}} J_i(Q)dQ$ electrons

Results of the unbiased algorithm

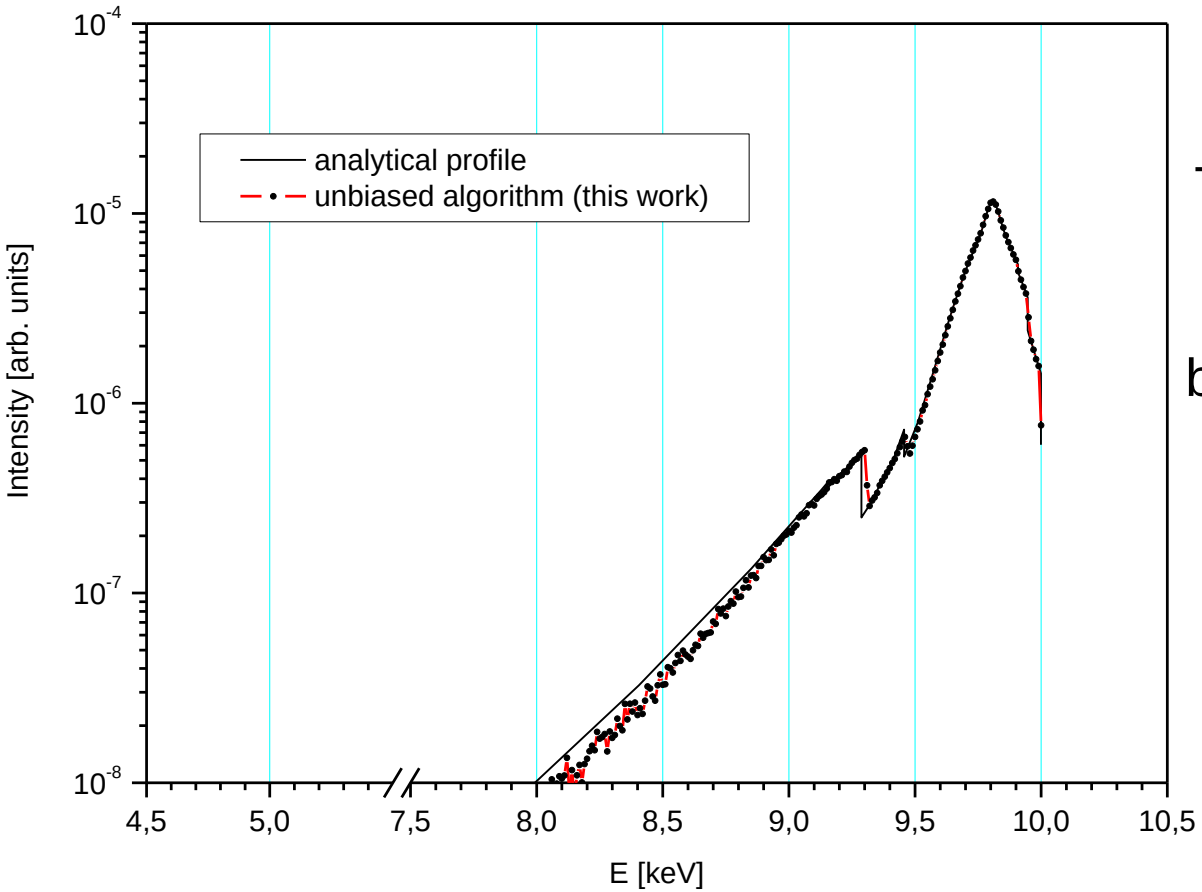

The deterministic code was essential to discover the wrong behaviour of the biased algorithm.

Summary

- Introduction
- Unbiased Monte Carlo simulation of the Compton Profile
- Deterministic vs Monte Carlo codes for transport calculations of line width effects
- Electron contributions to photon transport
- Conclusions

Deterministic vs Monte Carlo codes for transport calculations of line width effects

This example shows how a deterministic calculation has been used to compute the multiple scattering of Lorentzian characteristic lines

Applied Radiation and Isotopes 70 (2012) 550–555

Contents lists available at SciVerse ScienceDirect

Applied Radiation and Isotopes

journal homepage: www.elsevier.com/locate/apradiso

Deterministic and Monte Carlo codes for multiple scattering photon transport

Jorge E. Fernández [a,b,*], Viviana Scot [a]

[a] Laboratory of Montecuccolino (DIENCA) Alma Mater Studiorum University of Bologna, Italy
[b] Istituto Nazionale di Fisica Nucleare (INFN), Italy

Condition to fulfill in order to produce photoelectric effect

$$E_0 \geq E_{absorption\ \ edge}$$

Mechanism for producing XRF lines

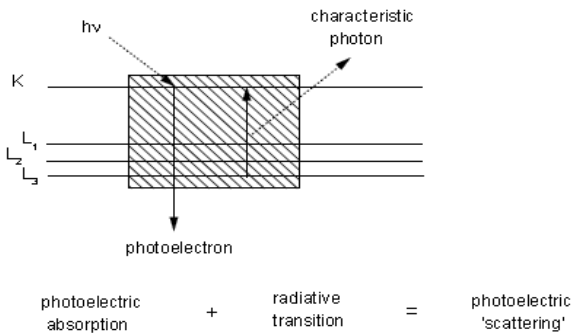

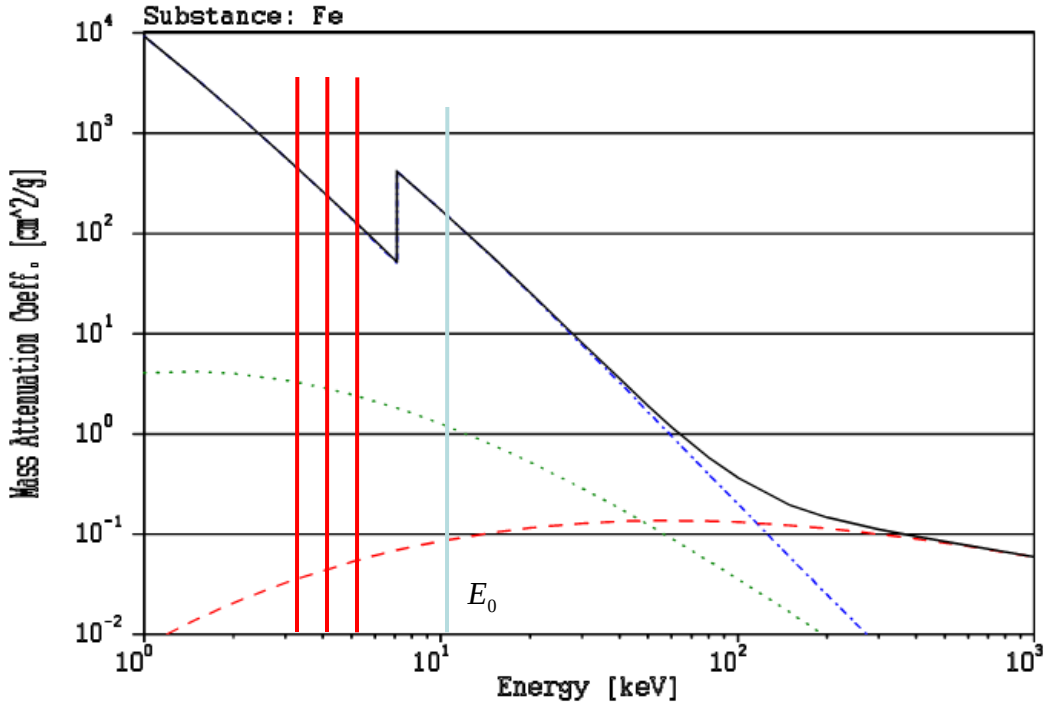

The width of the atomic levels is responsible for the natural width of the lines

$$\underbrace{\Gamma}_{\substack{\textit{total}\\ \textit{transition}\\ \textit{width}}} = \sum_k \underbrace{\Gamma_k}_{\substack{\textit{subshell}\\ \textit{level}\\ \textit{width}}}$$

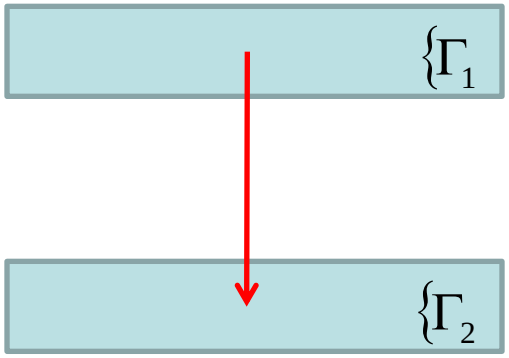

$$\Gamma = \Gamma_1 + \Gamma_2$$

The widths of the atomic levels are the recommended values in Campbell and Papp, *At. Data and Nucl. Data Tables* **77**, 1–56 (2001)

Lorentzian shape of the line

$$\ell(E,E_\ell;\gamma_{E_\ell}) = \frac{1}{\pi}\frac{\frac{\Gamma_{E_\ell}}{2}}{\left((E-E_\ell)^2+\left(\frac{\Gamma_{E_\ell}}{2}\right)^2\right)} = \frac{1}{\pi}\frac{\gamma_{E_\ell}}{\left((E-E_\ell)^2+\gamma_{E_\ell}{}^2\right)}$$

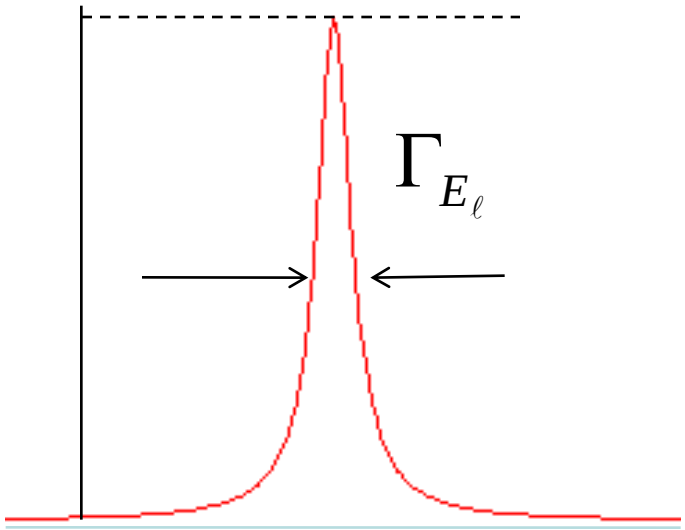

sometimes is used the
Half Width at Half Maximum (HWHM)

$$\gamma_{E_\ell} = \Gamma_{E_\ell}/2$$

Emission of a Lorentzian K-line

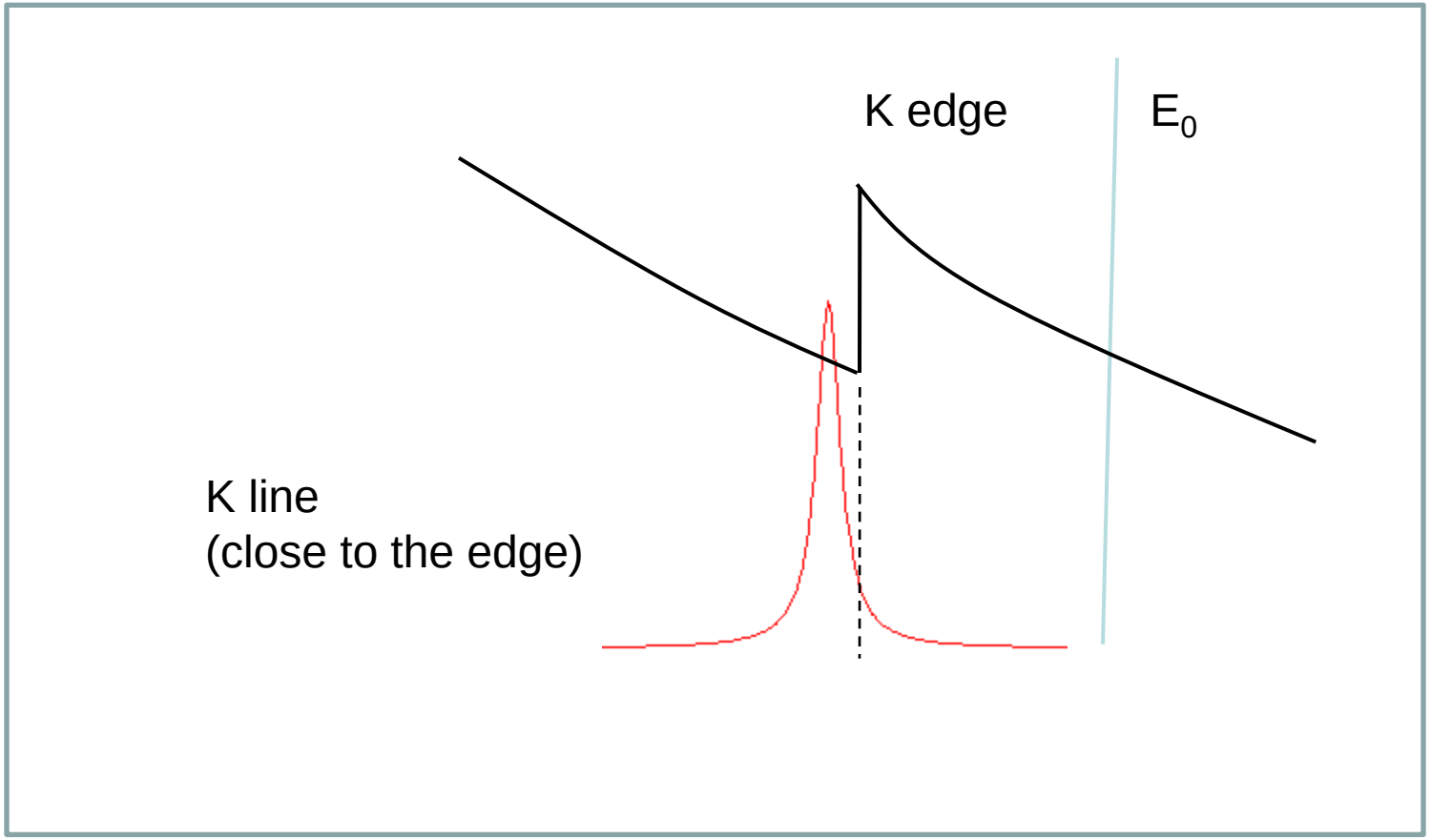

Transport kernel for a Lorentzian line (wavelength regime)

$$k_{P_{\lambda_i}}(\vec{\omega},\lambda,\vec{\omega}',\lambda')\Big|_L = \frac{1}{4\pi} Q_{\lambda_i}(\lambda')\,\ell(\lambda,\lambda_i;\gamma_{\lambda_i})\,[1-\mathrm{U}(\lambda'-\lambda_{e_i})]\,\mathrm{U}(\lambda-\lambda')$$

Emission probability

Energy conservation

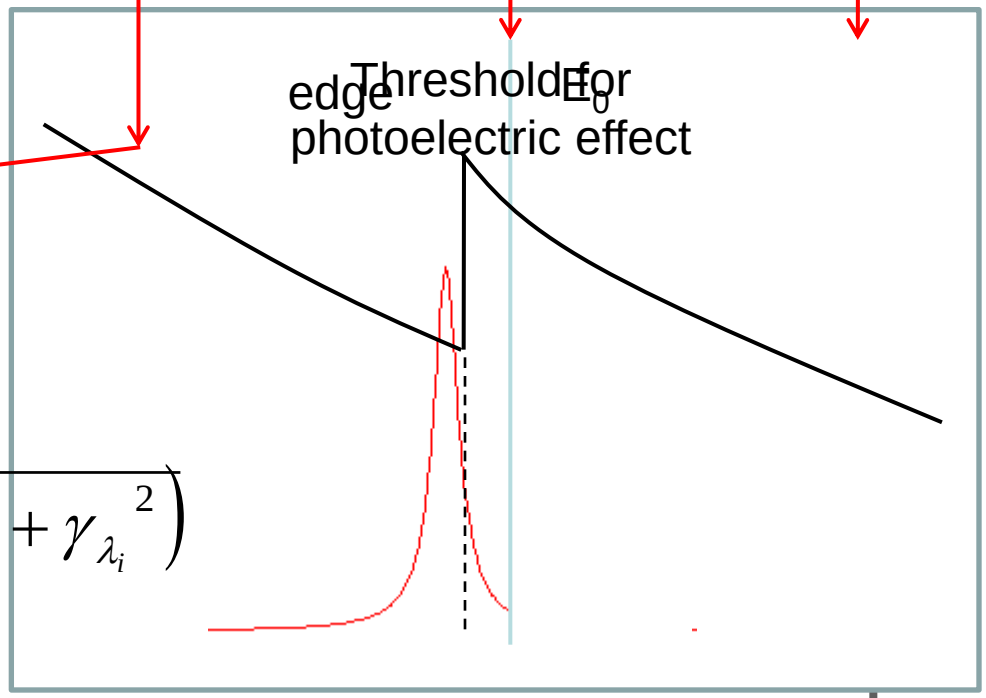

Lorentzian distribution

$$\ell(\lambda,\lambda_i;\gamma_{\lambda_i}) = \frac{1}{\pi}\frac{\gamma_{\lambda_i}}{\left((\lambda-\lambda_i)^2+\gamma_{\lambda_i}{}^2\right)}$$

MC vs Deterministic description of a Lorentzian line

✓In MC the energy of the characteristic photon is randomly sampled at every interaction using a Lorentzian distribution centered at E_0.

✓One interesting effect appears when the Lorentzian tail crosses the edge, i.e. the energy of the emitted photon is high enough to produce another vacancy and, therefore, a self-enhancement effect.

✓Since the high energy tail has always a very low probability, this case requires refined variance reduction techniques in order to get significant results.

✓The slow asymptotic decrease of the Lorentzian distribution introduces a further complication to describe multiple scattering with reasonable statistics.

✓Therefore, we propose to use instead a deterministic method based on the wavelength (energy) discretization of the Lorentzian distribution.

Discretization of the Lorentzian distribution (wavelength regime)

We define a new normalized distribution between the finite limits $\left[-(2t+1)\gamma_i, (2t+1)\gamma_i\right]$

$$\ell_\nu(\lambda, \lambda_i; \gamma_{\lambda_i}) = \frac{1}{\nu\pi} \frac{\gamma_{\lambda_i}}{\left((\lambda - \lambda_i)^2 + \gamma_{\lambda_i}{}^2\right)}$$

where $$\nu = \int_{\lambda_i - (2t+1)\gamma_i}^{\lambda_i + (2t+1)\gamma_i} \ell(\lambda, \lambda_i; \gamma_{\lambda_i})\, d\lambda = \frac{2}{\pi} \arctan(2t+1)$$

and use a discrete δ-expansion for the Lorentzian

$$\ell_\nu(\lambda, \lambda_i; \gamma_{\lambda_i}) = \sum_{k=-t}^{t} p_k\, \delta\left(\lambda - \left[\lambda_i + 2k\gamma_i\right]\right)$$

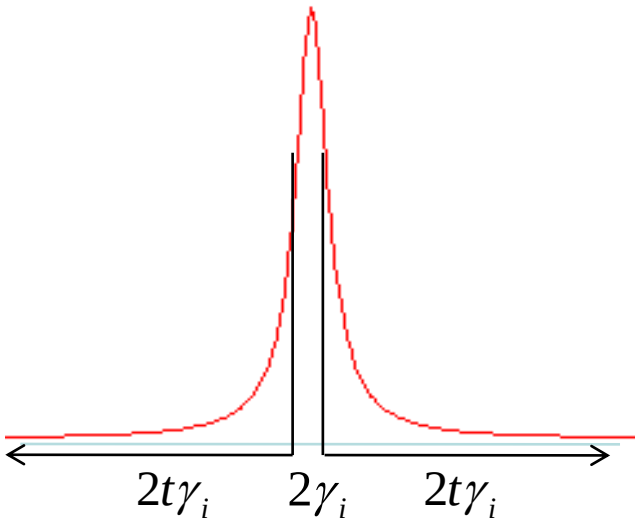

with coefficients

$$p_k = \int_{\lambda_i + 2k\gamma_i - \gamma_i}^{\lambda_i + 2k\gamma_i + \gamma_i} \ell_\nu(\lambda, \lambda_i; \gamma_{\lambda_i})\, d\lambda$$

$$= \frac{1}{\nu\pi}\left[\arctan(2k+1) - \arctan(2k-1)\right] \quad , \quad (k = -t..t)$$

Discretized kernel for the Lorentzian line (wavelength regime)

$$k_{P_{\lambda_i}}(\vec{\omega},\lambda,\vec{\omega}',\lambda')\Big|_L = \frac{1}{4\pi} Q_{\lambda_i}(\lambda') \sum_{k=-t}^{t} p_k \, \delta\left(\lambda-\lambda_{ik}\right)[1-\mathrm{U}(\lambda'-\lambda_{e_i})]\mathrm{U}(\lambda-\lambda')$$

$$= \frac{1}{4\pi} Q_{\lambda_i}(\lambda')[1-\mathrm{U}(\lambda'-\lambda_{e_i})] \sum_{k=k_{\min}}^{t} p_k \, \delta\left(\lambda-\lambda_{ik}\right)$$

with

$$\lambda_{ik} = \lambda_i + 2k\gamma_i$$

$$k_{\min} = \max\left[-t, -\left|\frac{\lambda_i-\lambda'}{2\gamma_i}\right|\right]$$

(energy conservation cut-off)

Primary XRF intensity of a Lorentzian line

The primary intensity of the line centered at the peak wavelength λ_i for an infinite thickness specimen is computed within an infinitely large acquisition window

$$I_{\lambda_i}^{(1)}(0,\vec{\omega})\Big|_L = \frac{I_0}{4\pi}|\eta| Q_{\lambda_i}(\lambda_0)[1-\mathrm{U}(\lambda_0-\lambda_{e_i})]\sum_{k=k_0}^{t}\frac{p_k}{\mu_{ik}|\eta_0|+\mu_0|\eta|}$$

where

$$k_0 = \max\left[-t, -\left|\frac{\lambda_i-\lambda_0}{2\gamma_i}\right|\right]$$

$$\mu_{ik} = \mu(\lambda_{ik})$$

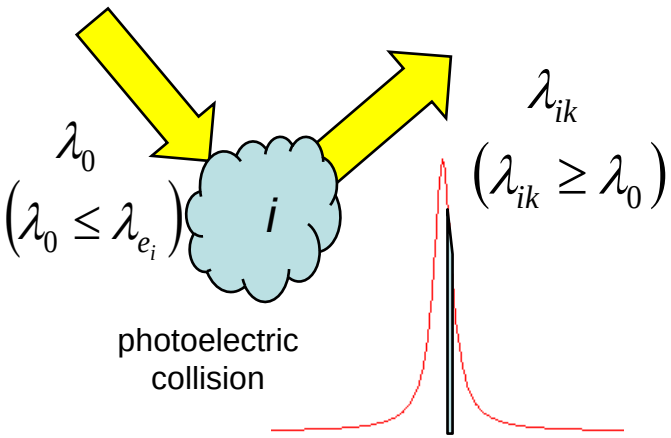

Secondary XRF intensity of a Lorentzian line

The secondary intensity of the line centered at the peak wavelength λ_i for an infinite thickness specimen is computed within an infinitely large acquisition window.

$$I_{\lambda_i}^{(2)}(0,\vec{\omega})\Big|_L = \frac{I_0}{8\pi}|\eta| \sum_{j}^{all\ lines} Q_{\lambda_j}(\lambda_0)[1-\mathrm{U}(\lambda_0-\lambda_{e_j})] \sum_{s=s\min_j(\lambda_0)}^{t} p_s\, Q_{\lambda_i}(\lambda_{js})[1-\mathrm{U}(\lambda_{js}-\lambda_{e_i})]$$

$$\sum_{k=k_{\min_i}(\lambda_{js})}^{t} \frac{p_k}{\mu_{ik}|\eta_0|+\mu_0|\eta|}\left[\frac{|\eta|}{\mu_{ik}}\ln\left(1+\frac{\mu_{ik}}{\mu_{js}|\eta|}\right)+\frac{|\eta_0|}{\mu_0}\ln\left(1+\frac{\mu_0}{\mu_{js}|\eta_0|}\right)\right]$$

$$k_{\min_i}(\lambda_{js}) = \max\left[-t,-\mathrm{Int}\left|\frac{\lambda_i-\lambda_{js}}{2\gamma_i}\right|\right]$$

$$s_{\min_j}(\lambda_0) = \max\left[-t,-\mathrm{Int}\left|\frac{\lambda_j-\lambda_0}{2\gamma_j}\right|\right]$$

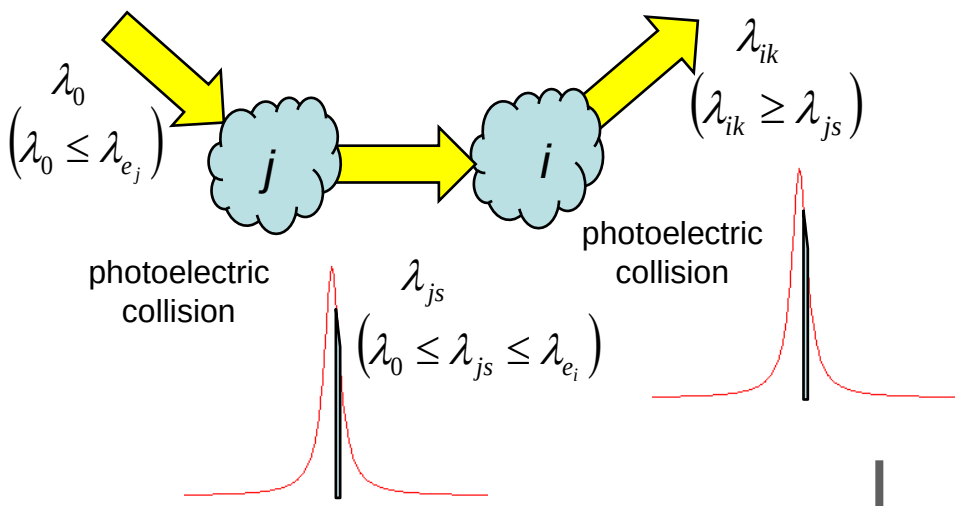

Example of almost symmetric Lorentzian lines

Sometimes the asymmetry is small …

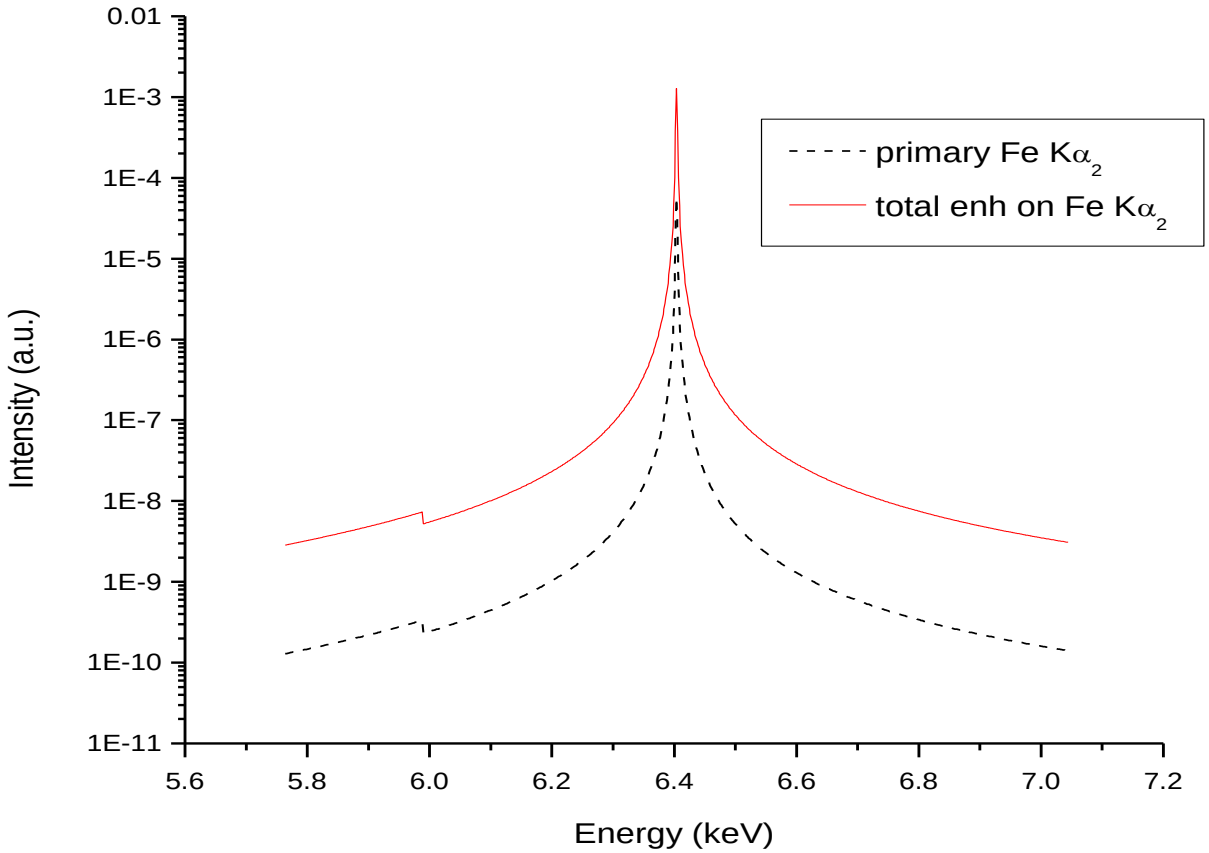

Secondary Lorentzian contributions can be very asymmetric

Sometimes the asymmetry is large …

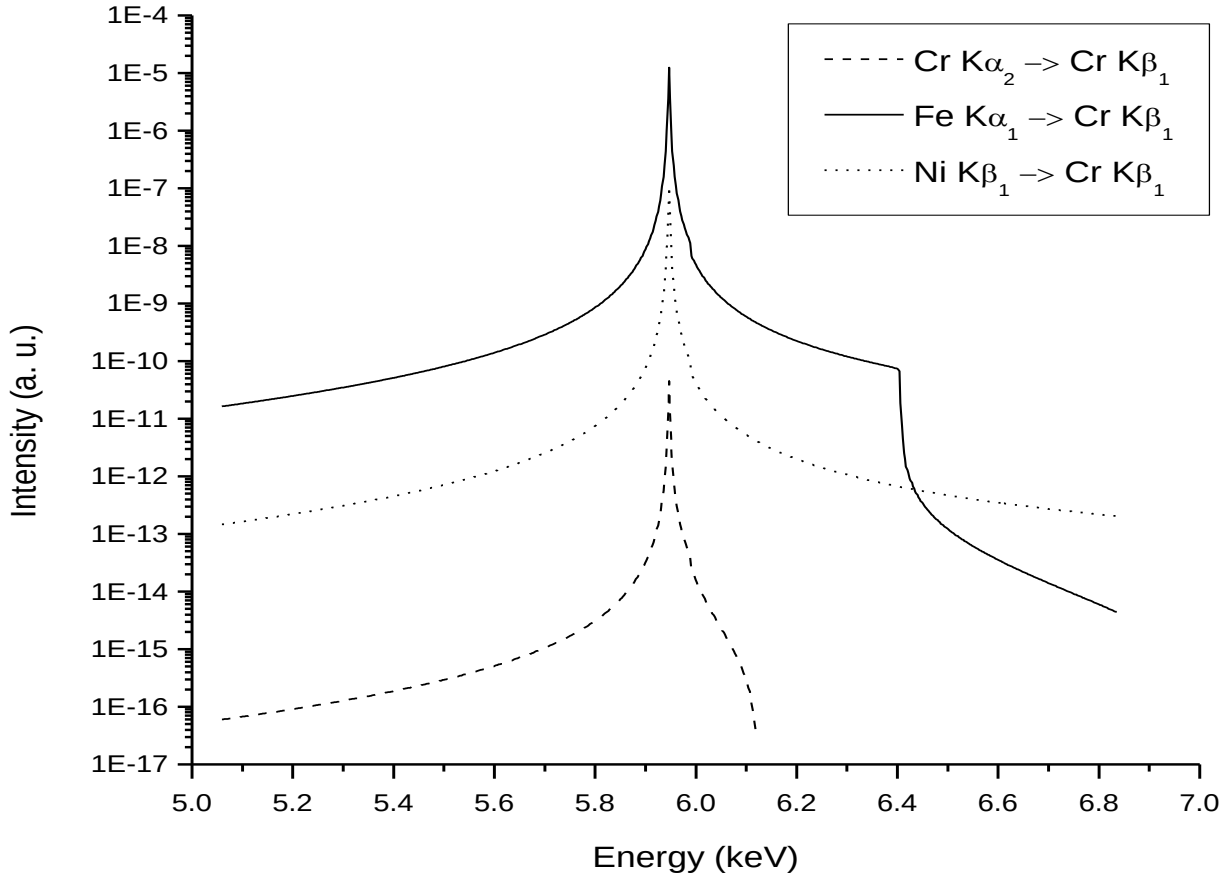

Summary

- Introduction
- Unbiased Monte Carlo simulation of the Compton Profile
- Deterministic vs Monte Carlo codes for transport calculations of line width effects
- Electron contributions to photon transport
- Conclusions

Electron contributions to photon transport

- The aim is to evaluate the contribution due to electrons to be included in photon transport codes without solving the complete coupled problem.
- The code PENELOPE (coupled electron-photon Monte Carlo) was used to study the effect of secondary electrons into the photon transport.
- The ad-hoc code KERNEL was developed to simulate a forced first collision at the origin of coordinates. We considered a point source of monochromatic photons.
- The physics of the interaction was described using the PENELOPE subroutine library.
- All the secondary electrons were followed along their multiple-scattering until their energy become lower of a predefinite threshold value.
- All photons produced by the electrons at every stage were accumulated.
- Polarization was not considered at this stage.

Prevailing photon interactions in the X-ray regime

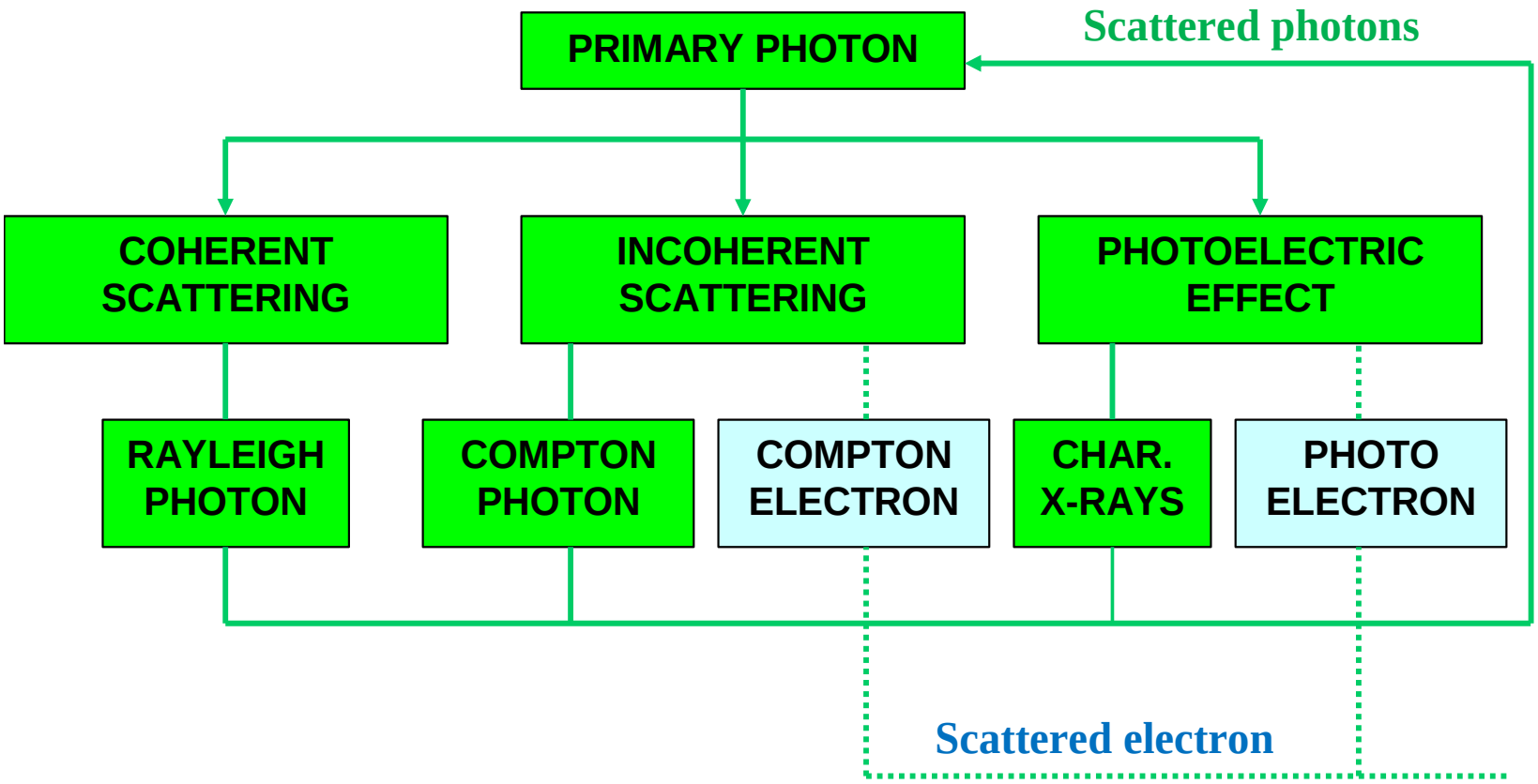

Electron-photon coupling

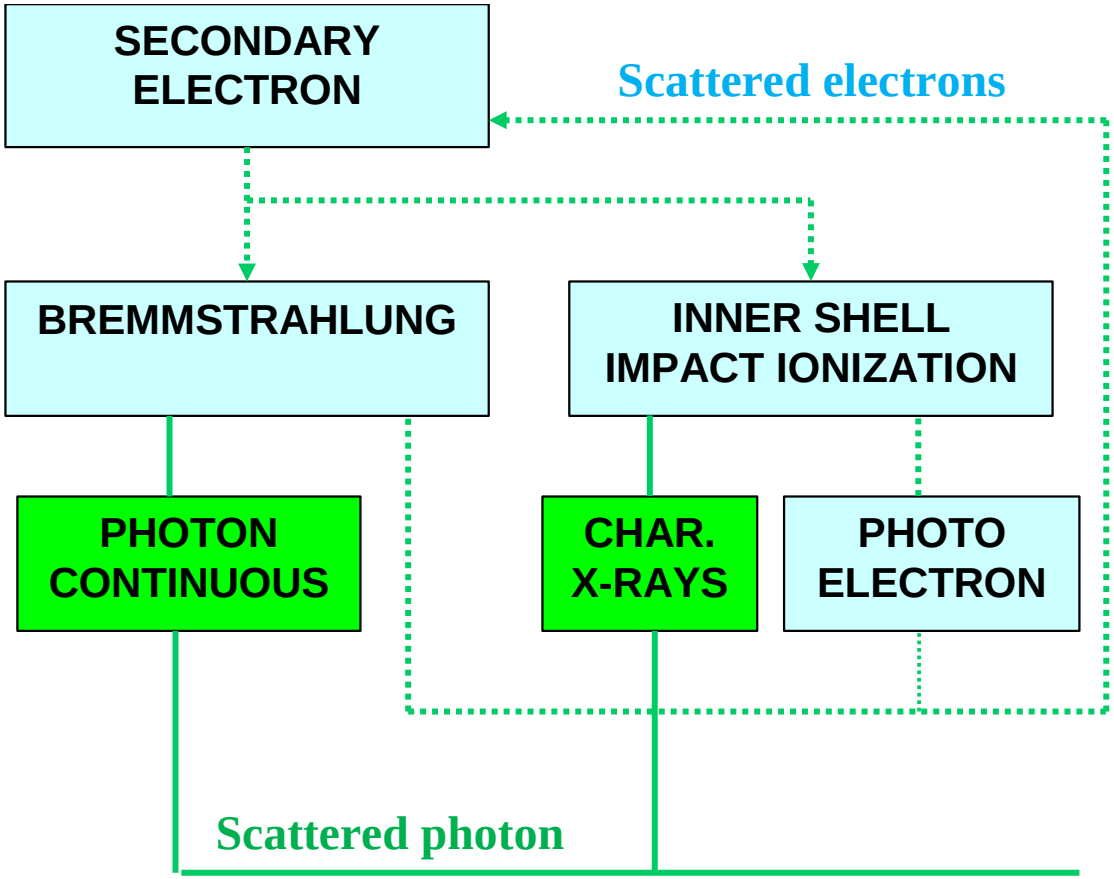

Description of the KERNEL code

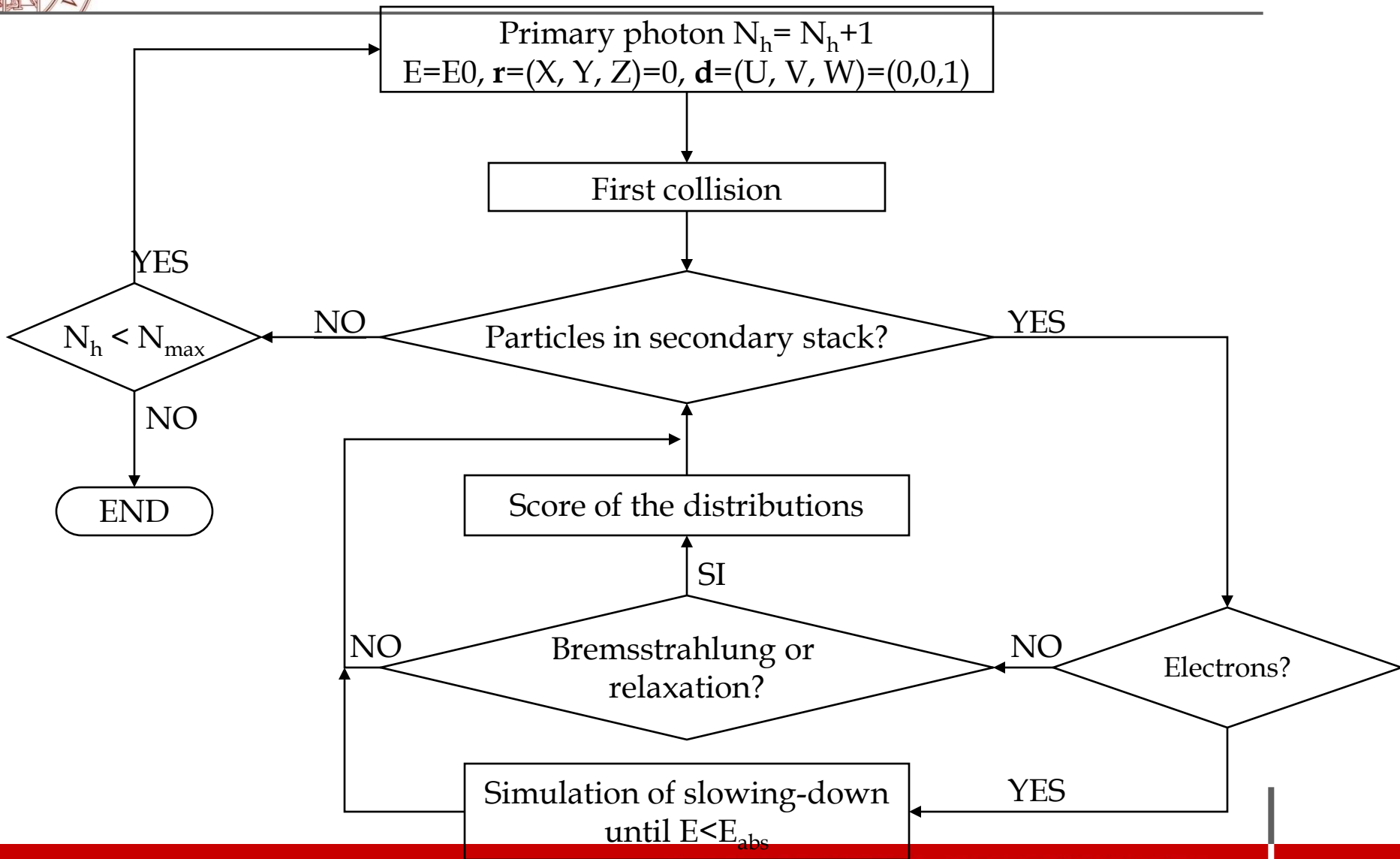

Types of electron contribution to photon transport

- Inner shell impact ionization: modifies the intensity of the characteristic lines

- Bremsstrahlung: contributes a continuous distribution

Inner shell impact ionization

This example shows how a MC simulation of electron-photon transport (SLOW) has been used to create an approximated kernel (FAST) to be used in photon transport codes.

Research article

X-RAY SPECTROMETRY

Accepted: 21 December 2012

Published online in Wiley Online Library: 22 May 2013

(wileyonlinelibrary.com) DOI 10.1002/xrs.2473

Electron contribution to photon transport in coupled photon-electron problems: inner-shell impact ionization correction to XRF

Jorge E. Fernandez,[a]* Viviana Scot,[a] Luca Verardi[b] and Francesc Salvat[c]

Polar angular distribution
Inner-shell impact ionization

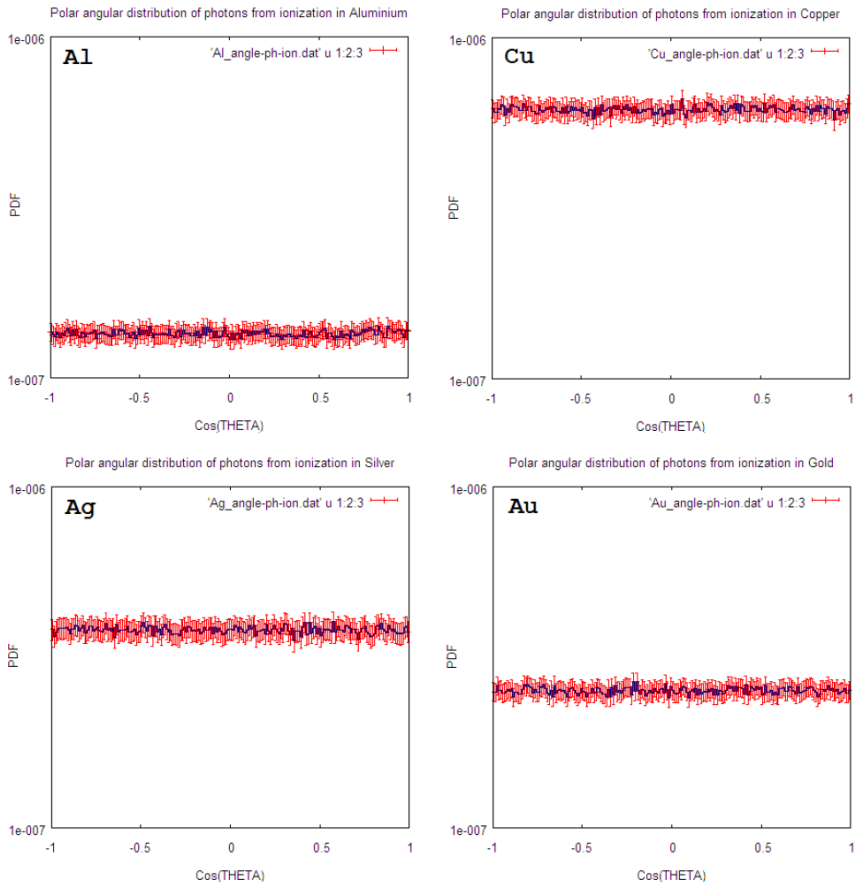

- ✓Primary photon source is 100 keV.
- ✓Blue lines denote computed values, red symbols are error bars.
- ✓The emission is isotropic.

Spatial distribution (1)
Electron range vs photon MFP

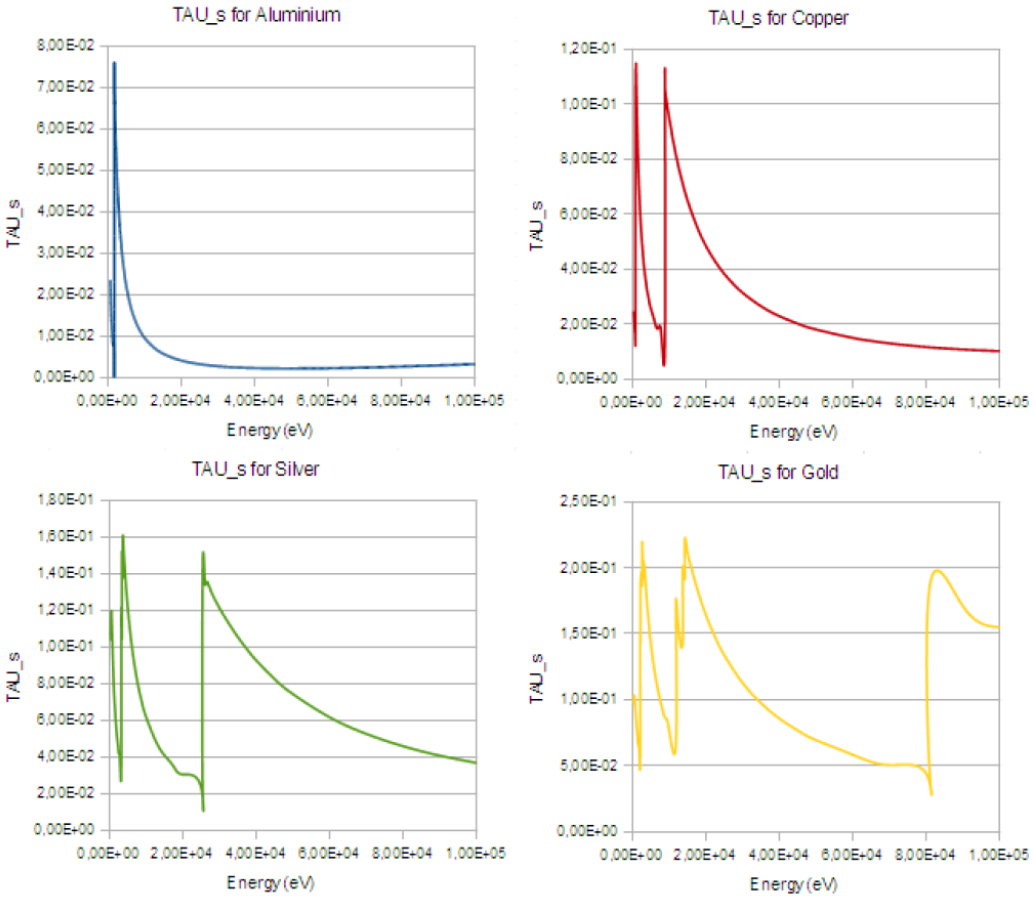

✓Parameter $\tau_s = R(E)/\lambda_p$

as a function of energy.

$R(E)$ Bethe range of electrons

λ_p Mean free-path of photons

✓Value ranges keep always small (order of 10^{-1}).

Spatial distribution (2)
Effective electron range

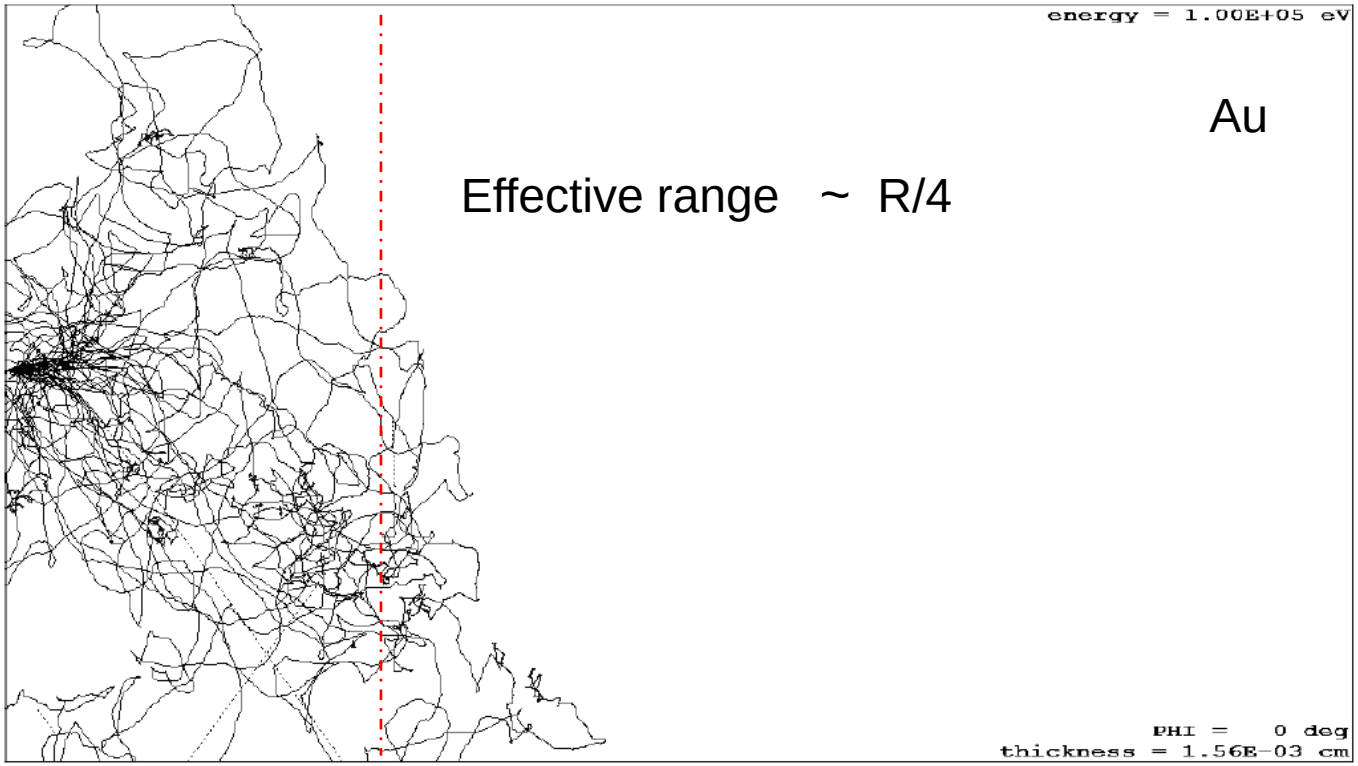

Bethe range

Photon emission
Inner shell impact ionization

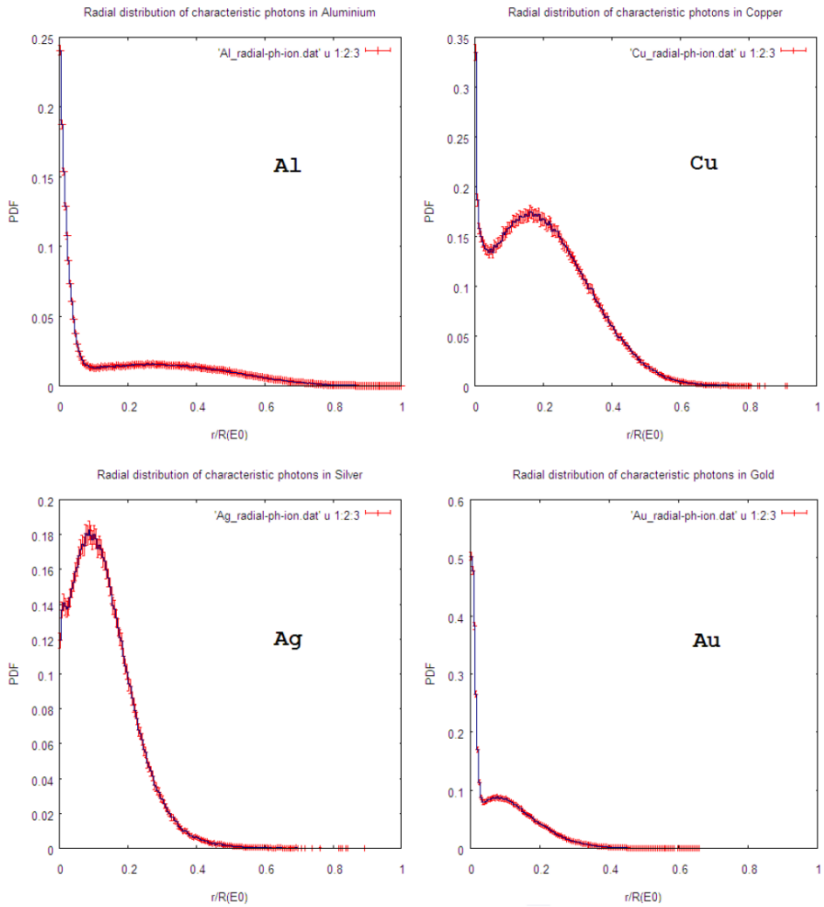

Radial distribution

- ✓Primary photon source is 100 keV.
- ✓Blue lines denote computed values, red symbols are error bars.
- ✓X-axis is r/R
- ✓All distributions keep below R/3

Photon emission
Inner shell impact ionization

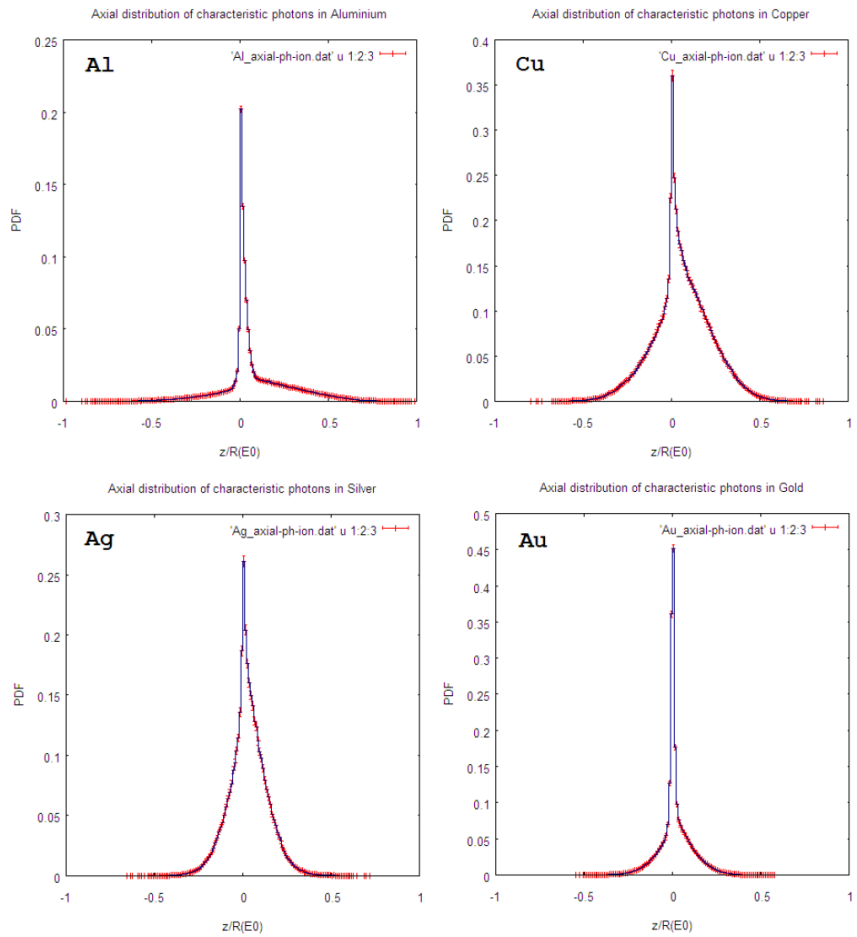

Axial distribution

- ✓Primary photon source is 100 keV.
- ✓Blue lines denote computed values, red symbols are error bars.
- ✓X-axis is z/R
- ✓All distributions keep below R/3

The correction as a function of energy

- Calculations were performed for all the lines of the elements Z=11-92 in the energy range 1-150 keV.
- Since the electrons loose their energy more efficiently in the low energy range, the computed contribution is higher for low energy lines.
- To compute the correction for a generic energy the whole interval was divided into 5 energy regions. The best fit of the energy correction at each energy interval was computed using 4 coefficients.

Electron correction on K-lines

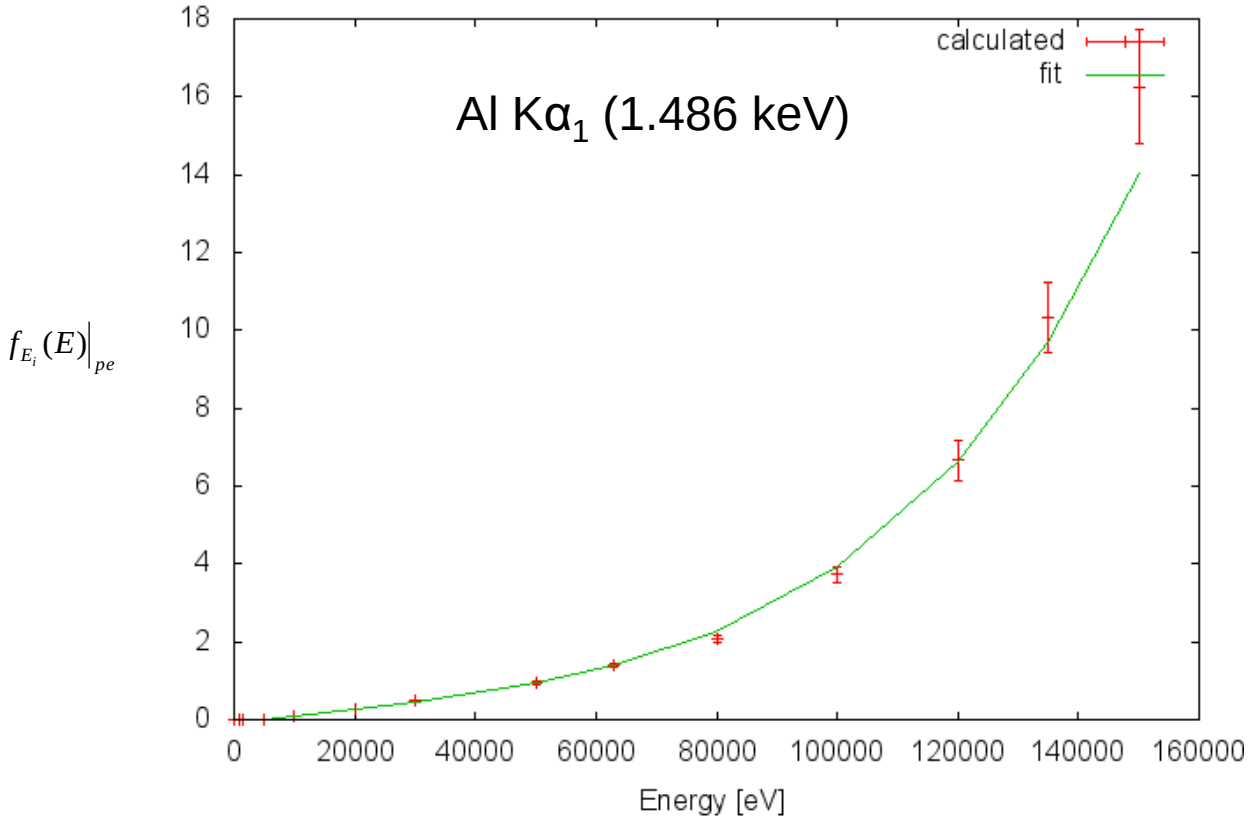

Low Z (11-20)

Na - Ca

Best fit

$$f_{E_i}(E)\big|_{pe} = \exp\left(\sum_{k=0}^{3} \alpha_k \ln(E)^k\right)$$

Electron correction on L-lines

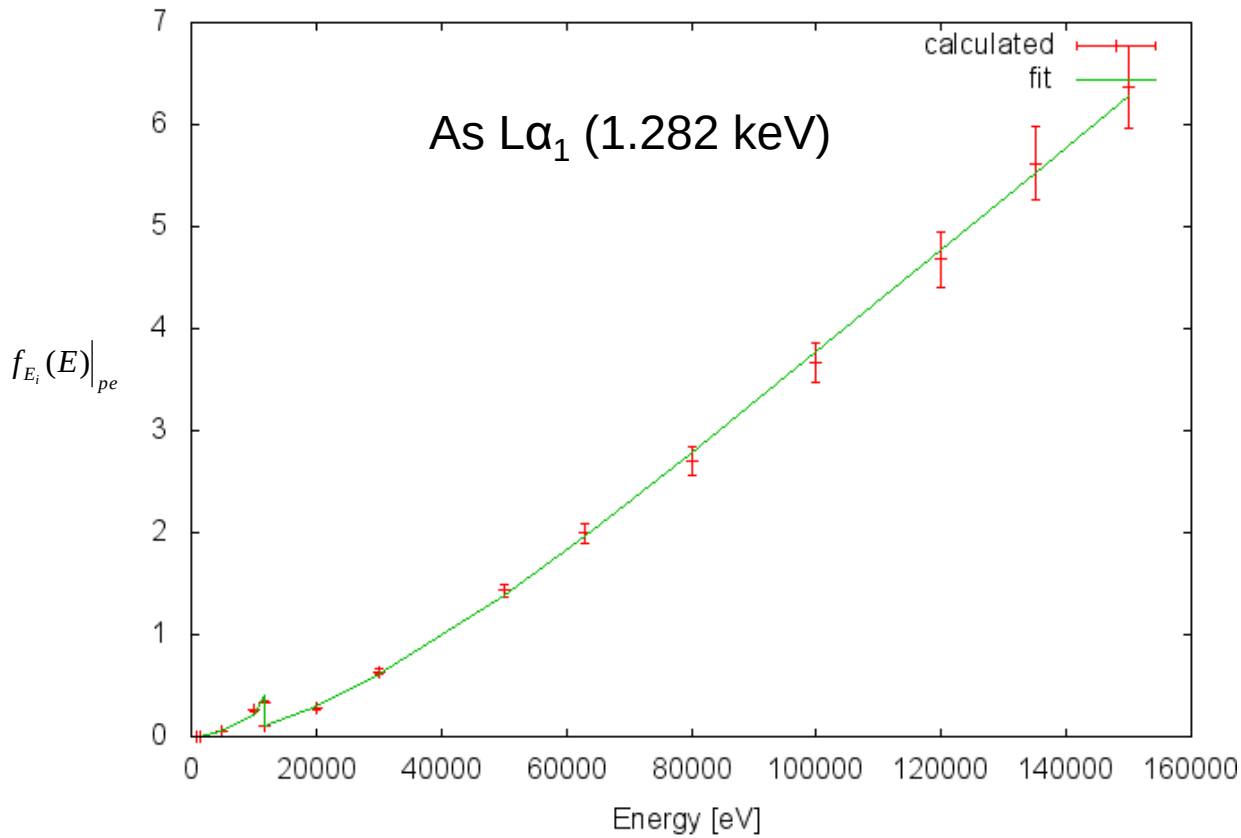

Medium Z (30-50)

Zn - Sn

Best fit

$$f_{E_i}(E)\big|_{pe} = \exp\left(\sum_{k=0}^{3} \alpha_k \ln(E)^k\right)$$

Electron correction on M-lines

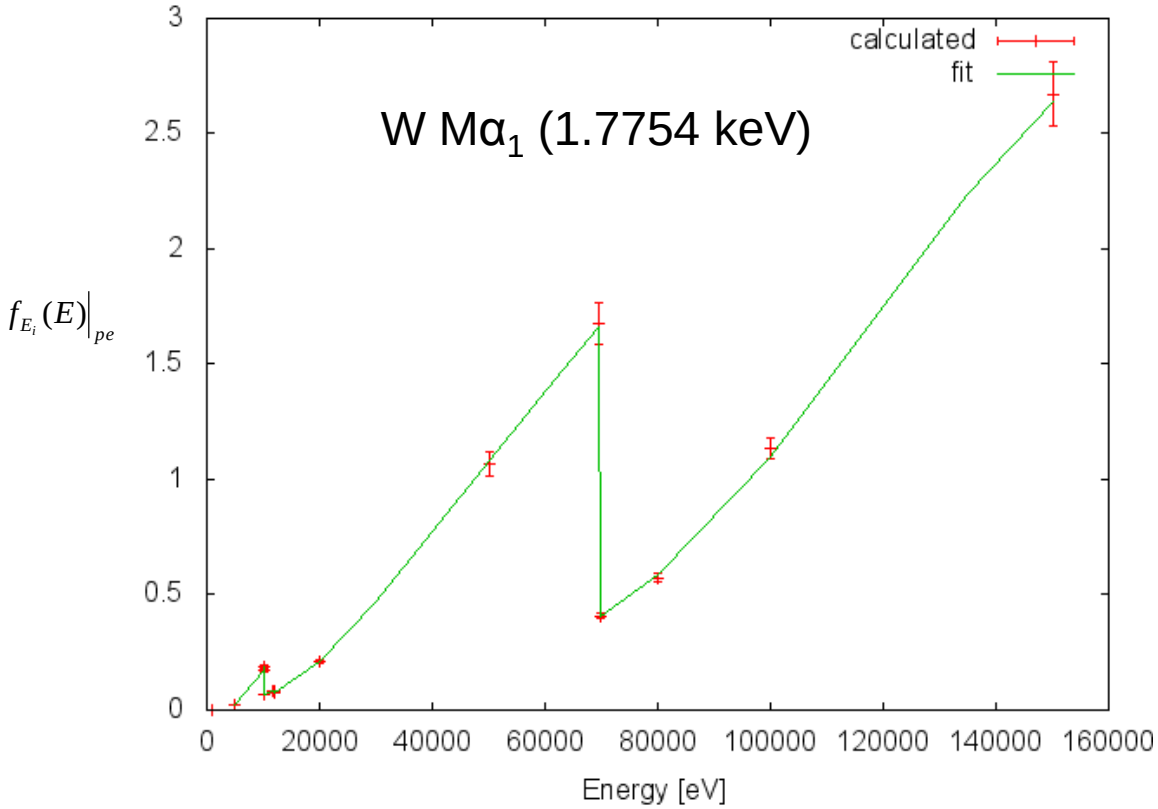

High Z (62-92)

Sm - U

Best fit

$$f_{E_i}(E)\big|_{pe} = \exp\left(\sum_{k=0}^{3} \alpha_k \ln(E)^k\right)$$

Kernel correction due to inner shell impact ionization

$$\Delta k_{P_{\lambda_i}}(\vec{\omega},\lambda,\vec{\omega}',\lambda')\Big|_{electron} = \frac{1}{4\pi} Q_{\lambda_i}(\lambda')\Big|_{electron} \delta(\lambda'-\lambda_i)\,[1-\mathrm{U}(\lambda'-\lambda_{e_i})]$$

- To avoid data-base differences between PENELOPE and other transport codes the electron correction $f_{\lambda_i}(\lambda')\big|_{pe}$ is computed in units of the photon contribution $Q_{\lambda_i}(\lambda')$.

$$\Delta k_{P_{\lambda_i}}(\vec{\omega},\lambda,\vec{\omega}',\lambda')\Big|_{electron} = \frac{1}{4\pi} \boxed{f_{\lambda_i}(\lambda')\big|_{pe}} Q_{\lambda_i}(\lambda')\,\delta(\lambda'-\lambda_i)\,[1-\mathrm{U}(\lambda'-\lambda_{e_i})]$$

$$f_{\lambda_i}(\lambda')\big|_{pe} = \frac{Q_{\lambda_i}(\lambda')\big|_{electron}}{Q_{\lambda_i}(\lambda')}$$

Corrected kernel comprising electron contributions

$$k_{P_{\lambda_i}}(\vec{\omega},\lambda,\vec{\omega}',\lambda') = \frac{1}{4\pi} Q_{\lambda_i}(\lambda')\left(1+ f_{\lambda_i}(\lambda')\Big|_{pe}\right)\delta(\lambda'-\lambda_i)\,[1-\mathrm{U}(\lambda'-\lambda_{e_i})]$$

where $$Q_{\lambda_i}(\lambda') = \tau_s(\lambda')\, g_{e_i}(\lambda')\, p_{\lambda_i}$$

- To compute the correction for a generic energy the whole interval is divided into 5 regions.

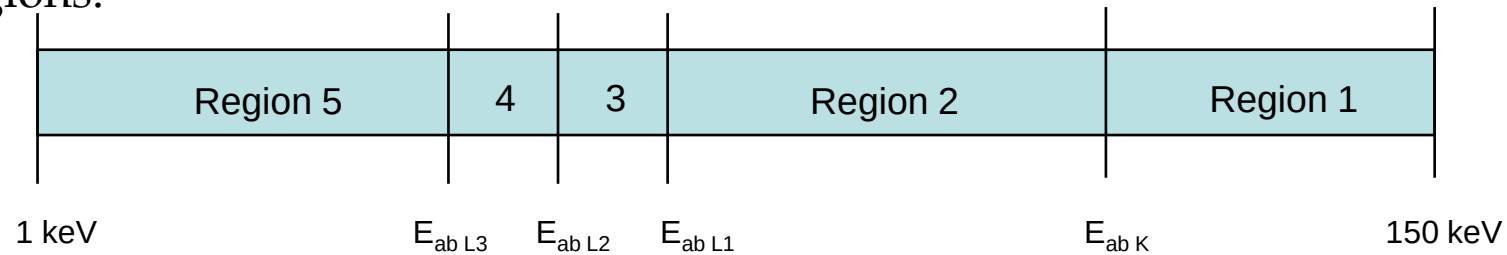

- The best fit of the energy correction at each energy interval requires 4 coefficients.

$$f_{\lambda_i}(\lambda')\Big|_{pe} = \exp\left(\sum_{k=0}^{3}\alpha_k \ln(E(\lambda'))^k\right)$$

Detailed calculation of inner shell impact ionization

Radiation Physics and Chemistry 95 (2014) 22–25

Contents lists available at ScienceDirect

Radiation Physics and Chemistry

journal homepage: www.elsevier.com/locate/radphyschem

Detailed calculation of inner-shell impact ionization to use in photon transport codes

Jorge E. Fernandez [a,*], Viviana Scot [a], Luca Verardi [b], Francesc Salvat [c]

Inner shell impact ionization correction is energy localized

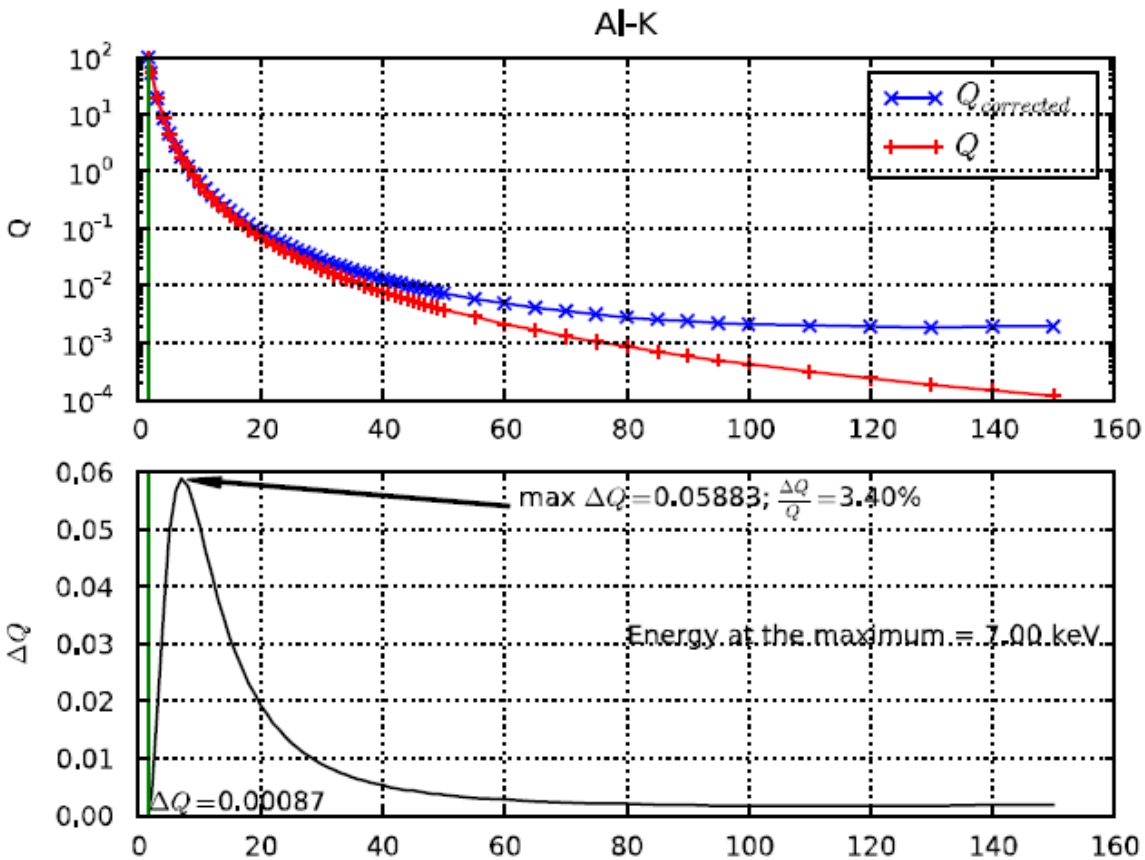

(1) To study ISII is necessary to measure at the proper energy

(2) The localization energy is element and line dependent

Inner shell impact ionization correction for K-lines

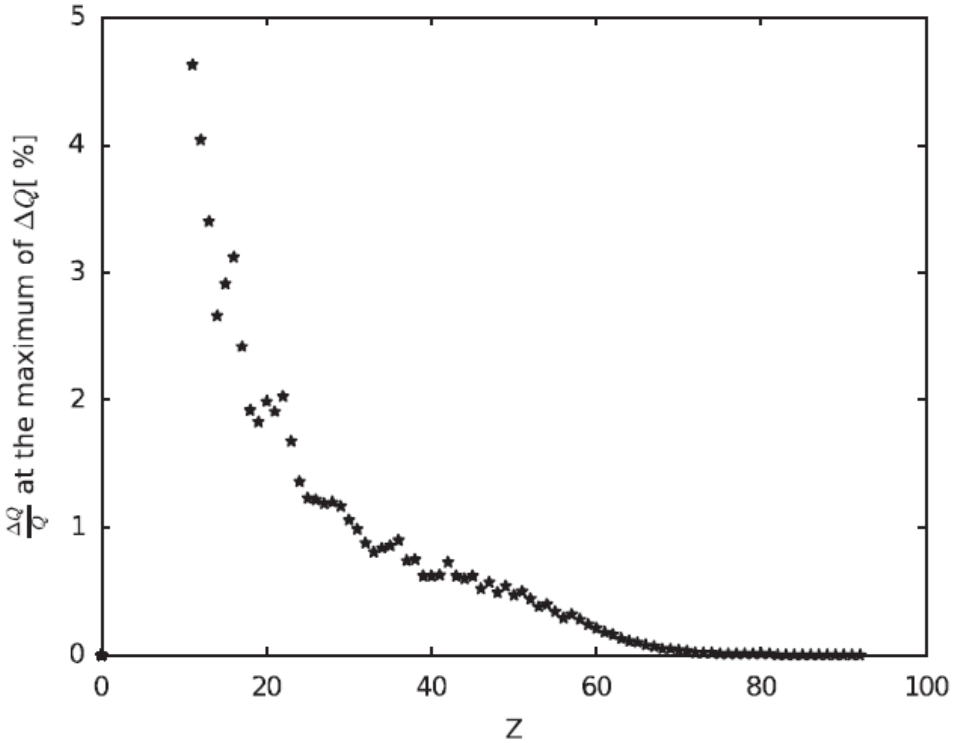

Fig. 4. Value of $\Delta Q/Q$ in %, at the energy of the maximum of ΔQ, as a function of the atomic number Z, for the K lines $K_{\alpha 1}$, $K_{\alpha 2}$, $K_{\beta 1}$. The value is the same for the three lines.

Inner shell impact ionization correction for L-lines

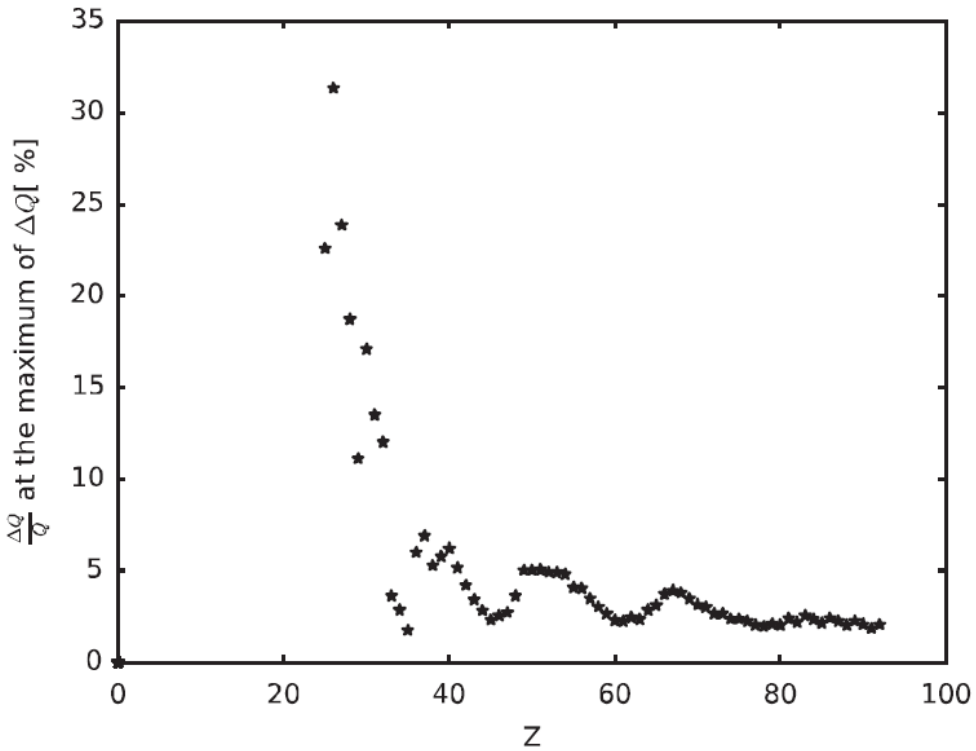

Fig. 5. Value of $\Delta Q/Q$ in %, at the energy of the maximum of ΔQ, as a function of the atomic number Z, for the most intense L lines: $L_{\alpha 1}$ and $L_{\alpha 2}$. The value is the same for both lines.

Types of electron contribution to photon transport

- Inner shell impact ionization: modifies the intensity of the characteristic lines

- Bremsstrahlung: contributes a continuous distribution

Obtained Result

The Bremsstrahlung correction was studied in terms of:

Spatial distribution

↓

The correction roughly occurs at the same place of the photon collision

Angular distribution

↓

The correction is isotropic

Energy distribution

↓

The correction depends on energy (wavelength)

Bremsstrahlung energy distribution

Example for a Fe target and 60 keV source energy

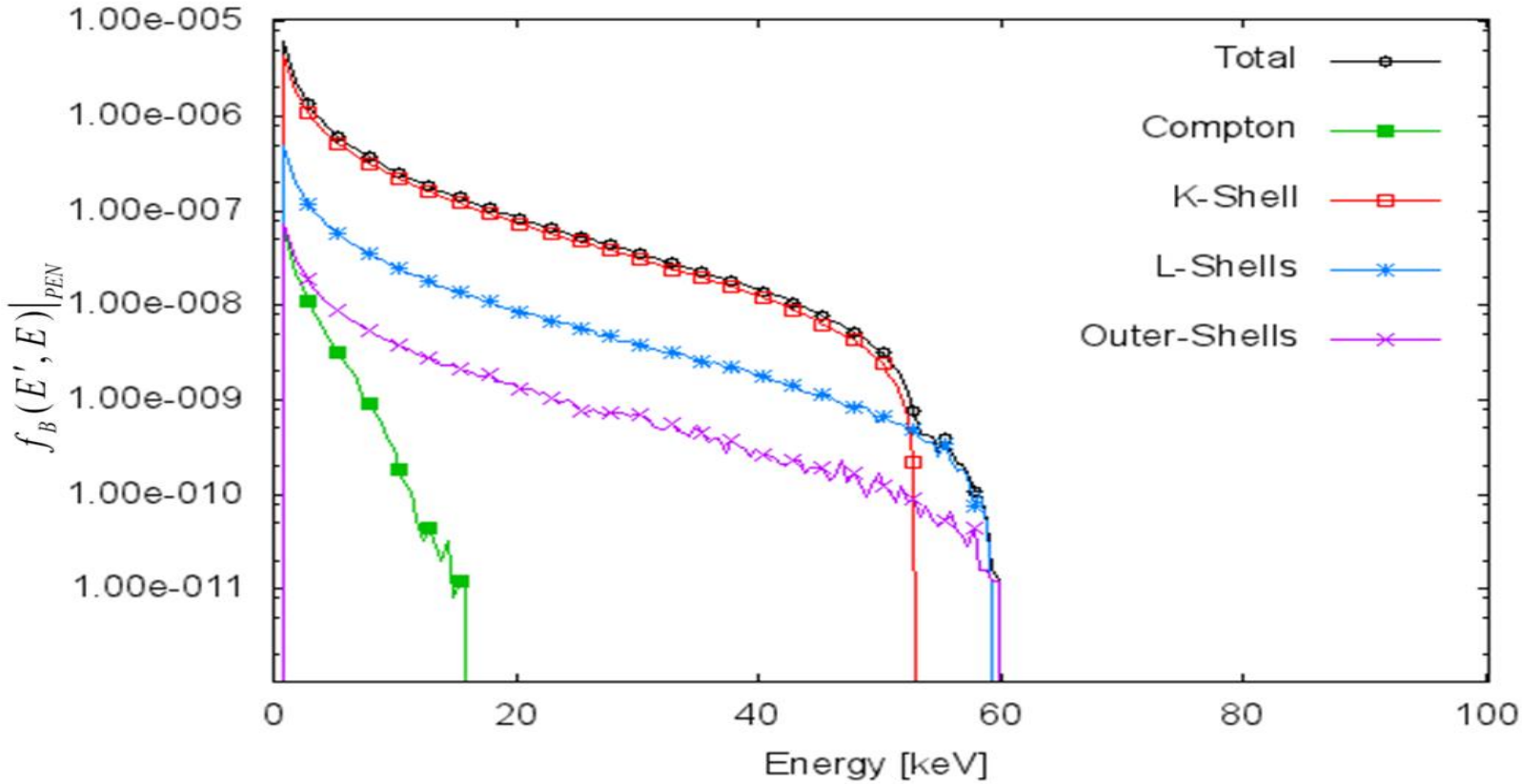

The Bremsstrahlung contribution was computed for all the different photon interactions which generate secondary electrons

Bremsstrahlung data library

It was created a data library comprising the energy distribution of the correction for selected source energy in the range 1-150 keV for all the elements with atomic numbers Z=1-92

Example of Bremsstrahlung distributions for a Fe target

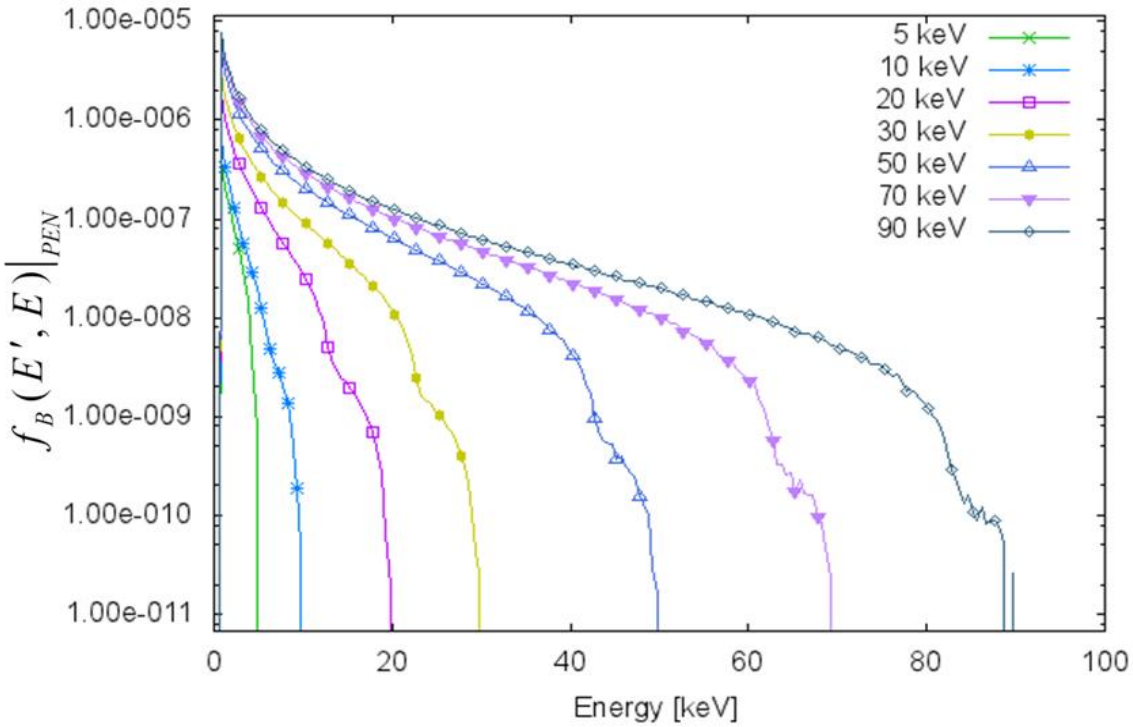

To avoid the discontinuities at the absorption edges

the Bremsstrahlung database includes the distributions for energies before and after the binding energy of each shell

Bremsstrahlung Kernel

The Bremsstrahlung correction can be added to the transport equation as a new kernel which gives a continuous distribution

$$k_B(\vec{\omega},\lambda,\vec{\omega}',\lambda') = \frac{1}{4\pi}\, f_B(\lambda',\lambda)$$

To avoid data-base differences between PENELOPE and other transport codes, the correction is computed in units of the Compton Scattering coefficient

$$\tilde{f}_B(\lambda',\lambda)\Big|_{PEN} = \frac{f_B(\lambda',\lambda)\big|_{PEN}}{\sigma_C(\lambda')\big|_{PEN}}$$

$$f_B(\lambda',\lambda) = \tilde{f}_B(\lambda',\lambda)\Big|_{PEN} \cdot \sigma_C(\lambda')$$

Data Library Interpolation

For a generic source energy *E'* the contribution is obtained by interpolating the created data library using an ad-hoc 2D interpolation scheme[1]:

Example of Bremsstrahlung library database interpolation for a Fe target with a 55 keV source energy

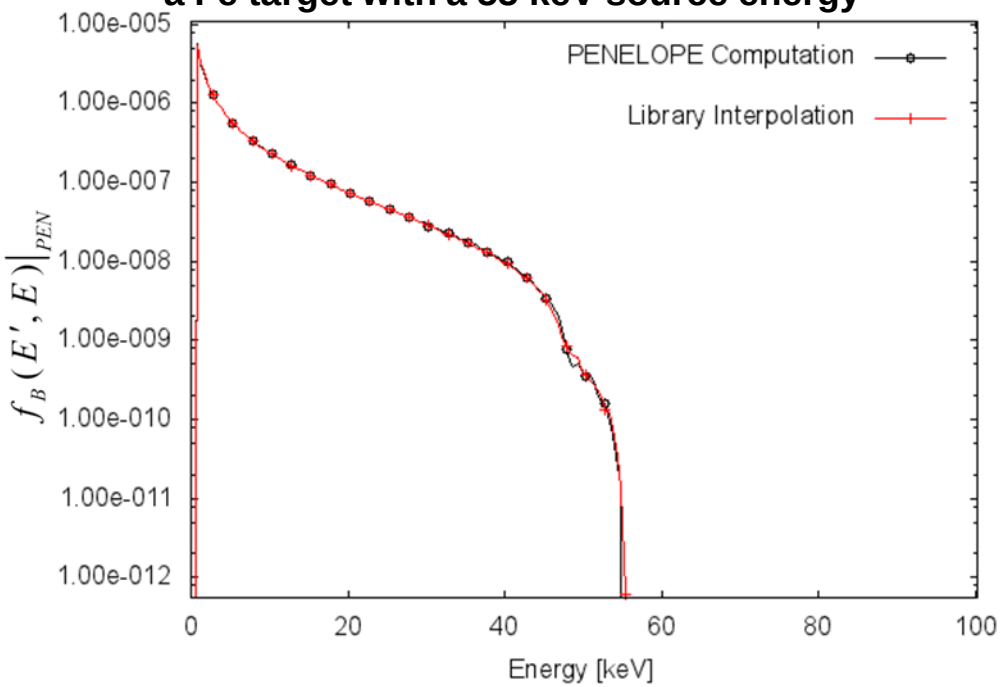

$$y(\bar{x}) = \frac{(E_2' - E')y_1(\bar{x}) + (E' - E_1')y_2(\bar{x})}{E_2' - E_1'}$$

with :

$$\bar{x} = x_1 \cdot \frac{E'}{E_1'}\,;\; x_1 = \bar{x} \cdot \frac{E_1'}{E'}\,;\; x_2 = \bar{x} \cdot \frac{E_2'}{E'}$$

$$y_1(\bar{x}) = f_B(E_1', x_1)\big|_{PEN}$$

$$y_2(\bar{x}) = f_B(E_2', x_2)\big|_{PEN}$$

[1] J.E. Fernandez, V. Scot, M. Badiali, A. Giudetti, Multiple scattering corrections for density profile unfolding from Compton signals in reflection geometry, X-Ray Spectrom., 36: 20-26 (2007). doi : 10.1002/xrs.2473

Mixture of Compounds

For composite materials with several species of atoms it is assumed that the overall contribution is obtained as a linear overlapping of the single elements corrections.

$$f_B(\lambda', \lambda)_{tot} = \sum_{i=1}^{N} w_i \cdot f_B(\lambda', \lambda)_i$$

Bremsstrahlung Simulation Results

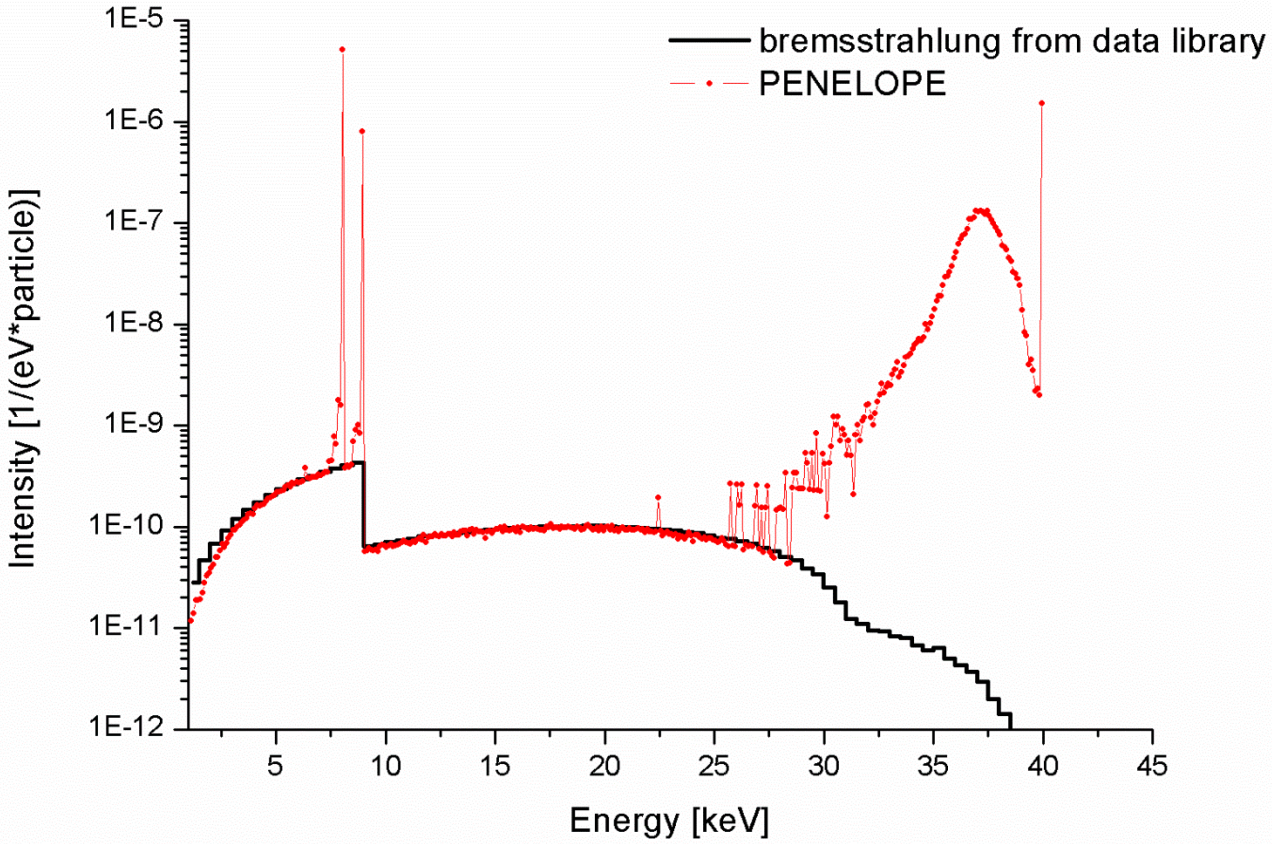

Comparison between the PENELOPE simulation and the first order intensity of bremsstrahlung computed using the data library. Sample is a Cu thin target. The source is a synchrotron beam at 40 keV. It is apparent the excellent agreement for bremsstrahlung. Speed improvement is 10^5

Spectrum Simulation Results (a)

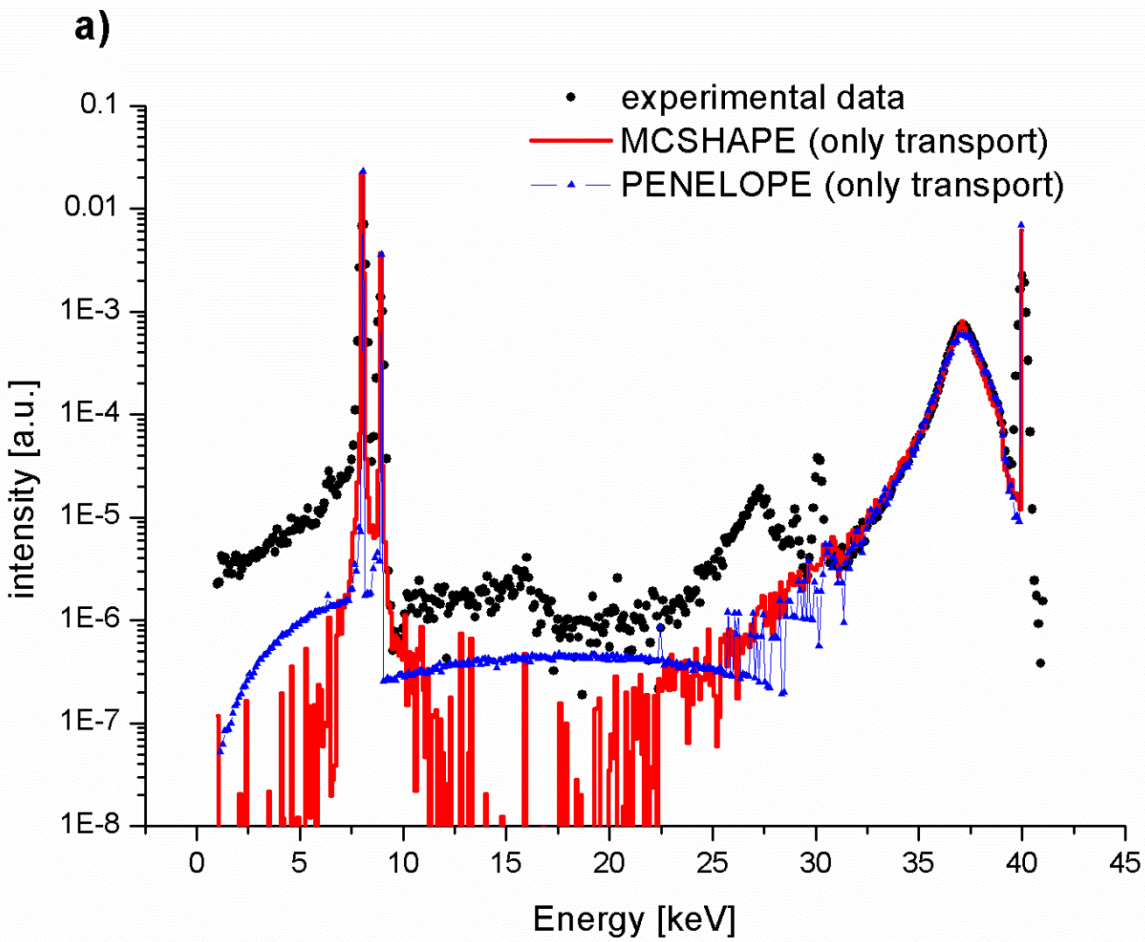

Comparison between PENELOPE and MCSHAPE simulations (only transport) computed using the data library and measurements. MCSHAPE not includes bremsstrahlung. Sample is a Cu thin target. The source is a synchrotron beam at 40 keV. Speed improvement is 10^5

Spectrum Simulation Results (b)

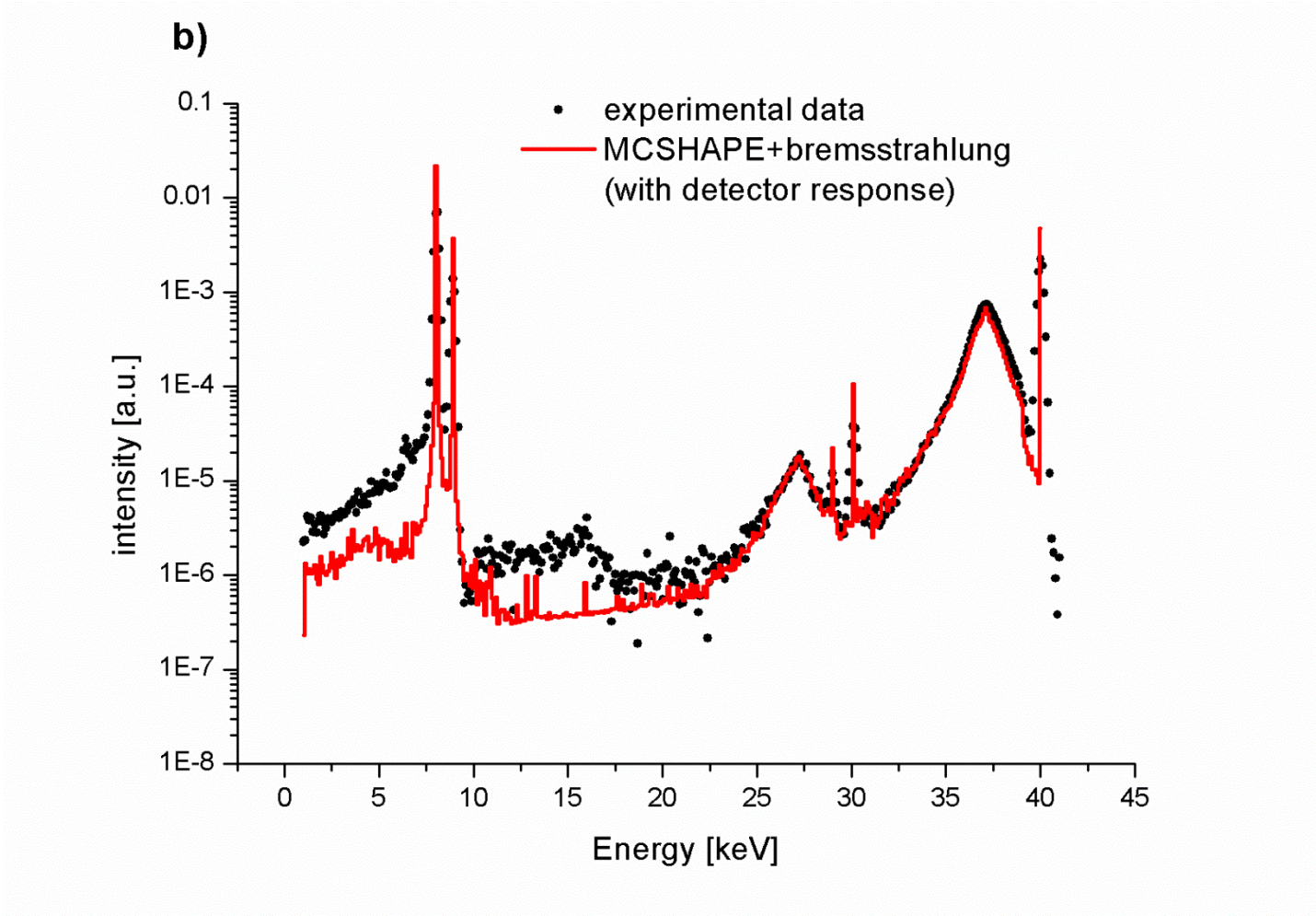

Comparison between MCSHAPE simulations computed using the data library and measurements. MCSHAPE includes bremsstrahlung and detector response. Sample is a Cu thin target. The source is a synchrotron beam at 40 keV.

Spectrum Simulation Results (c)

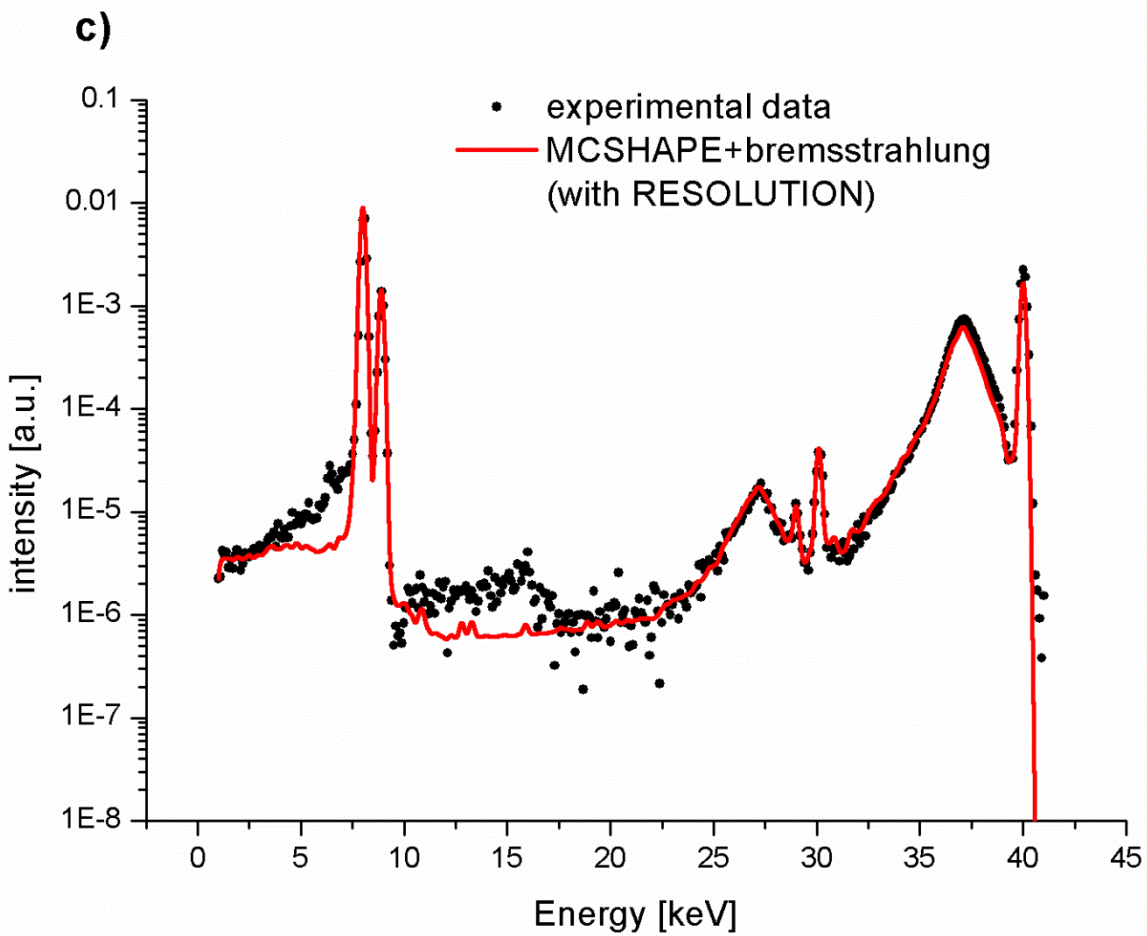

Comparison between MCSHAPE simulations computed using the data library and measurements. MCSHAPE includes bremsstrahlung, detector response and resolution. Sample is a Cu thin target. The source is a synchrotron beam at 40 keV.

Summary

- Introduction
- Unbiased Monte Carlo simulation of the Compton Profile
- Deterministic vs Monte Carlo codes for transport calculations of line width effects
- Electron contributions to photon transport
- Conclusions

Conclusions

Deterministic and Monte Carlo techniques demonstrate to be complementary to provide the best description of transport problems.

We have shown three different cases in photon transport to illustrate the symbiosis of MC and Deterministic approaches:

1) Deterministic calculations were essential to discover the wrong behaviour of a biased algorithm used to simulate the Compton profile in largely diffused MC codes.
2) Deterministic calculations provide a better framework to describe the influence of the Lorentzian breath on multiple scattering contributions to XRF lines.
3) Coupled photon-electron MC calculations were essential to obtain a simple correction of the photon kernel to include the effect of inner shell impact ionization and bremsstrahlung from electrons.
4) To obtain a good description of measurement it is necessary to include the detector response function (MCSHAPE in mode response) and a proper description of the resolution (postprocessing code RESOLUTION).

ALMA MATER STUDIORUM
UNIVERSITÀ DI BOLOGNA

Jorge Fernandez
jorge.fernandez@unibo.it